

Heavy-ball-based optimal thresholding algorithms for sparse linear inverse problems

Zhong-Feng Sun · Jin-Chuan Zhou · Yun-Bin Zhao

Received: date / Accepted: date

Abstract Linear inverse problems arise in diverse engineering fields especially in signal and image reconstruction. The development of computational methods for linear inverse problems with sparsity is one of the recent trends in this field. The so-called optimal k -thresholding is a newly introduced method for sparse optimization and linear inverse problems. Compared to other sparsity-aware algorithms, the advantage of optimal k -thresholding method lies in that it performs thresholding and error metric reduction simultaneously and thus works stably and robustly for solving medium-sized linear inverse problems. However, the runtime of this method is generally high when the size of the problem is large. The purpose of this paper is to propose an acceleration strategy for this method. Specifically, we propose a heavy-ball-based optimal k -thresholding (HBOT) algorithm and its relaxed variants for sparse linear inverse problems. The convergence of these algorithms is shown under the restricted isometry property. In addition, the numerical performance of the heavy-ball-based relaxed optimal k -thresholding pursuit (HBROTP) has been evaluated, and simulations indicate that HBROTP admits robustness for signal and image reconstruction even in noisy environments.

Keywords Sparse linear inverse problems · optimal k -thresholding · heavy-ball method · restricted isometry property · phase transition · image processing

Mathematics Subject Classification (2020) 94A12 · 15A29 · 90C25 · 90C20 · 49M20

The work was founded by the National Natural Science Foundation of China (NSFC 12071307 and 11771255), Young Innovation Teams of Shandong Province (2019KJII013), and Shandong Province Natural Science Foundation (ZR2021MA066, ZR2023MA020).

Zhong-Feng Sun
School of Mathematics and Statistics, Shandong University of Technology, Zibo, Shandong, China. E-mail: zfsun@sdut.edu.cn

Jin-Chuan Zhou
School of Mathematics and Statistics, Shandong University of Technology, Zibo, Shandong, China. E-mail: jinchuanzhou@sdut.edu.cn

Yun-Bin Zhao
Corresponding author. Shenzhen Research Institute of Big Data, Chinese University of Hong Kong, Shenzhen, Guangdong, China. E-mail: yunbinzhao@cuhk.edu.cn

1 Introduction

In recent years, the linear inverse problem has gained much attention in various fields such as wireless communication [10, 19] and signal/image processing [4, 9, 25, 26, 35, 43, 47, 52]. A typical linear inverse problem is about the reconstruction of unknown data $z \in \mathbb{R}^r$ from the acquired linear measurements

$$y = \Phi z + \nu, \quad (1.1)$$

where $\Phi \in \mathbb{R}^{m \times r}$ is a given measurement matrix, $y \in \mathbb{R}^m$ are the acquired measurements, and $\nu \in \mathbb{R}^m$ are the measurement errors. In this paper, we consider the case $m < r$, for which it is generally impossible to reconstruct the data z from the linear system (1.1) unless z possesses a certain structure such as sparsity. Fortunately, in many practical applications, the signal to recover possesses certain sparse structure or it can be sparsely represented under a suitable transformation. For instance, many natural image can be sparsely represented via wavelet transforms. Suppose that z can be sparsely represented via the basis $\Psi \in \mathbb{R}^{r \times n}$ ($r \leq n$), i.e., $z = \Psi x$ where the vector $x \in \mathbb{R}^n$ is either k -sparse or k -compressible for some integer number $k \ll n$. A vector is said to be k -sparse if $\|x\|_0 \leq k$, and k -compressible if x can be approximated by a k -sparse vector, where $\|\cdot\|_0$ denotes the number of nonzero entries of a vector. With a sparse representation of z , the model (1.1) can be written as

$$y = Ax + \nu, \quad (1.2)$$

where $A = \Phi\Psi \in \mathbb{R}^{m \times n}$ ($m < n$) is still referred to as a measurement matrix. In this case, the problem (1.1) is transformed to the so-called sparse linear inverse (SLI) problem which is to reconstruct the sparse data x via the linear system (1.2). Once the sparse data x is reconstructed, the original data z can be immediately obtained by setting $z := \Psi x$. The SLI problem can be formulated as an optimization problem (see, e.g., [4, 9, 25, 28, 19, 43, 49]). Typically, it can be formulated as the sparse optimization problem

$$\min_u \{\|y - Au\|_2^2 : \|u\|_0 \leq k\}. \quad (1.3)$$

It can also be formulated as the ℓ_1 -minimization (basis pursuit) problem

$$\min_u \{\|u\|_1 : Au = y\} \quad (1.4)$$

as well as the LASSO problem

$$\min_u \|y - Au\|_2^2 + \mu\|u\|_1, \quad (1.5)$$

where $\mu > 0$ is called a regularization parameter. All these models, (1.3)-(1.5), are widely used in signal and image reconstruction with sparsity.

Depending on the problem formulations, several classes of algorithms for SLI problems have been developed over the past decades, including the thresholding algorithms [25, 26, 28], greedy methods [20, 42, 48], convex optimization [14, 15, 18, 57], nonconvex optimization [17], and Bayesian methods [45, 51]. In this paper, we focus on the model (1.3) for which the thresholding algorithms are particularly convenient to develop. The thresholding method was first proposed by Donoho and Johnstone [23]. It has experienced a significant development since 1994 and has

evolved into a large family of algorithms which includes the hard thresholding [6, 8, 9, 27, 33, 38], soft thresholding [21, 22, 24] and optimal k -thresholding algorithms [56, 58]. It is worth stressing that an advantage of thresholding methods is that the algorithms can guarantee the generated points being feasible to the problem (1.3). The simplest thresholding method might be the iterative hard thresholding (IHT) [8]. The combination of IHT and orthogonal projection yields the hard thresholding pursuit (HTP) [27]. Due to low computational complexity, IHT and HTP have been widely used in signal reconstruction with compressive samplings [6, 7, 9, 33].

However, as pointed out in [56, 58], performing hard thresholding on non-sparse iterates may not necessarily reduce the objective value of (1.3) and thus may cause numerical oscillation during iterations. Thus the optimal k -thresholding operator was introduced in [56] (see also [58]) to alleviate such a weakness of hard thresholding. This operator may perform thresholding on iterates and, in the meantime, reduce the objective value of (1.3). The optimal k -thresholding (OT) and optimal k -thresholding pursuit (OTP) algorithms are first developed in [56]. Recall that the optimal k -thresholding of a given vector $v \in \mathbb{R}^n$ is defined as

$$\min_w \{\|y - A(v \circ w)\|_2^2 : \mathbf{e}^T w = k, w \in \{0, 1\}^n\}, \quad (1.6)$$

where $\mathbf{e} = (1, 1, \dots, 1)^T \in \mathbb{R}^n$, $\{0, 1\}^n$ is the set of n -dimensional binary vectors and $v \circ w := (v_1 w_1, \dots, v_n w_n)^T$ denotes the Hadamard product of two vectors. However, from a computational point of view, it is generally more convenient to solve the following convex optimization

$$\min_w \{\|y - A(v \circ w)\|_2^2 : \mathbf{e}^T w = k, 0 \leq w \leq \mathbf{e}\}, \quad (1.7)$$

which is a tight relaxation of (1.6). This problem is referred to as data compressing problem in [56, 58]. Based on (1.7), the relaxed optimal k -thresholding (ROT ω) and relaxed optimal k -thresholding pursuit (ROTP ω) algorithms were proposed in [56, 58], where ω represents times of data compression that are performed in the algorithms. When $\omega = 1$, the algorithm is termed as ROTP. Some modifications of ROTP using partial gradient and Newton-type search direction were studied recently in [39, 40]. While the convex optimization (1.7) can be efficiently solved by existing convex optimization solvers, however, solving such a problem remains time-consuming when the size of the problem is large. Thus it is important to study how the computational cost of ROTP-type methods might be reduced and how these methods can be accelerated by integrating an acceleration technique such as the heavy-ball (HB) or Nesterov's technique. By using linearization together with a certain binary regularization method, the so-called nature thresholding (NT) algorithm is developed recently in [59], whose computational complexity is significantly lower than that of ROTP ω since the NT algorithm is able to avoid solving any optimization problem like (1.7). In this paper, we investigate the ROTP-type algorithms from the acceleration perspective by showing that the HB technique is able to improve the performance of the ROTP-type algorithms.

The HB method introduced by Polyak [44] can be seen as a two-step method which combines the momentum term and gradient descent direction. In recent years, HB has found wide applications in image processing, data analysis, distributed optimization and undirected networks [3, 31, 32, 34, 36, 41, 50, 53]. The theoretical analysis (global convergence and local convergence rate) for HB methods

has been investigated by several researchers. For example, the linear convergence rate of HB for unconstrained convex optimization problem was established by Aujol et. al [3]; Mohammadi et. al [41] analyzed the relation between the convergence rate of HB and its variance amplification when the objective function of the problem is strongly convex and quadratic; Xin and Khan [53] showed that the distributed HB method with appropriate parameters attains a global R -linear rate, and it has potential acceleration compared with some first-order methods for ill-conditioned problems. Other acceleration techniques including the Nesterov's one can be found in [32,34,36,41].

In this paper, we merge the optimal k -thresholding and HB acceleration technique to form the following algorithms for the SLI problem formulated as (1.3):

- Heavy-ball-based optimal k -thresholding (HBOT),
- Heavy-ball-based optimal k -thresholding pursuit (HBOTP),
- Heavy-ball-based relaxed optimal k -thresholding (HBROT ω),
- Heavy-ball-based relaxed optimal k -thresholding pursuit (HBROT $P\omega$),

where the integer parameter ω denotes the number of times for solving (1.7) at every iteration. The global convergence of these algorithms is established in this paper under the restricted isometry property (RIP) introduced by Candès and Tao [14], and the main results are summarized in Theorems 1 and 2. The performances of HBROT P (i.e., HBROT $P\omega$ with $\omega = 1$) and several existing algorithms such as ROTP2 [56], partial gradient ROTP (PGROT P) [40], ℓ_1 -minimization [18], orthogonal matching pursuit (OMP) [25,48] and projected linearized Bregman method (PLB) [11] are compared through numerical experiments. The phase transition with Gaussian random data is adopted to demonstrate the performances of the proposed algorithms for SLI problems.

The algorithm development for linear inverse problems is usually model-based in the sense that different formulations of the problem require different algorithms. The ℓ_1 -minimization method is naturally applied to the model (1.4) and a more general convex optimization solver can be directly used to handle the LASSO problem (1.5). However, ℓ_1 -minimization and LASSO solvers are not convenient to solve the problem (1.3) for which a thresholding method might be more suitable. The optimal k -thresholding method is proposed to enhance the success rates and stability of existing hard thresholding algorithms. Unlike ℓ_1 -minimization and LASSO solvers, the hard or optimal k -thresholding procedures can reconstruct any prescribed (interested) k significant components of the target signals without the need to reconstruct the whole signal. Also, recent study in [59] indicates that a certain modification of the optimal k -thresholding method may lead to a fast and efficient algorithm which has far lower computational cost than most existing algorithms including ℓ_1 -minimization and LASSO solvers. Thus a further study of the optimal k -thresholding algorithms on their acceleration, simplification and modification remains interesting and important from both viewpoints of practical applications and algorithmic development itself.

While our discussion in this paper is focused on hard/optimal thresholding algorithms, it is worth briefly mentioning the class of soft thresholding methods which is widely used for signal processing as well. The soft thresholding method can be derived in different ways. Taking the model (1.4) as an example, a soft thresholding method can be developed from the Bregman regularization framework [54], which involves solving the convex subproblem (1.5) at each iteration.

Based on (1.5), using linearization and ℓ_2 -proximity can lead to the linearized Bregman (LB) methods [13, 54, 55], which is a class of soft thresholding methods. Moreover, linearization combined with Krylov subspace projection can also yield a soft thresholding method such as the PLB in [11]. Other soft thresholding methods can be found in [4, 10, 37]. The soft thresholding method needs to select a regularization parameter, but how to select such a parameter so that the algorithm can guarantee to solve a SLI problem remains an open question. The numerical experiments in Sections 5.1 and 5.3 indicate that the HBROT algorithm proposed in this paper might be more stable and robust than ℓ_1 -minimization and PLB for data reconstruction in many cases.

This paper is organized as follows. In Section 2, we introduce some notations, definitions, useful inequalities and algorithms. In Section 3, we discuss the error bounds and convergence of HBOT and HBOTP under the RIP. The error bounds for HBROT ω and HBOTP ω are given in Section 4. Numerical results from synthetic signals and real images are reported in Section 5.

2 Preliminary and algorithms

2.1 Notations

Denote by $N := \{1, 2, \dots, n\}$. Given a subset $\Omega \subseteq N$, $\overline{\Omega} := N \setminus \Omega$ denotes the complement set of Ω and $|\Omega|$ denotes its cardinality. For a vector $z \in \mathbb{R}^n$, the support of z is represented as $\text{supp}(z) := \{i \in N : z_i \neq 0\}$, and the vector $z_\Omega \in \mathbb{R}^n$ is obtained by zeroing out the elements of z supported on $\overline{\Omega}$ and retaining those supported on Ω . Given the sparse level k , $\mathcal{L}_k(z)$ denotes the index set of the k largest absolute entries of z . As usual, $\mathcal{H}_k(z) := z_{\mathcal{L}_k(z)}$ is called the hard thresholding of z . The symbols $\|\cdot\|_1$ and $\|\cdot\|_2$ represent ℓ_1 -norm and ℓ_2 -norm of a vector, respectively. Throughout the paper, \mathbf{e} denotes the vector of ones. \mathcal{W}^k and \mathcal{P}^k are two sets in \mathbb{R}^n defined as

$$\mathcal{W}^k = \{w \in \mathbb{R}^n : \mathbf{e}^T w = k, w \in \{0, 1\}^n\}, \quad \mathcal{P}^k = \{w \in \mathbb{R}^n : \mathbf{e}^T w = k, 0 \leq w \leq \mathbf{e}\}.$$

2.2 Definitions and basic inequalities

Let us first recall the restricted isometry property (RIP) of a matrix and the optimal k -thresholding operator $Z_k^\#(\cdot)$.

Definition 1 [14] Given a matrix $A \in \mathbb{R}^{m \times n}$ with $m < n$, the k th order restricted isometry constant (RIC) of A , denoted by δ_k , is the smallest nonnegative number δ such that

$$(1 - \delta)\|u\|_2^2 \leq \|Au\|_2^2 \leq (1 + \delta)\|u\|_2^2 \quad (2.1)$$

for all k -sparse vectors $u \in \mathbb{R}^n$. The matrix A is said to satisfy the RIP of order k if $\delta_k < 1$.

Definition 2 [56, 58] Given a vector $u \in \mathbb{R}^n$, let $w^*(u)$ be the solution of the binary optimization problem

$$\min_w \left\{ \|y - A(u \circ w)\|_2^2 : w \in \mathcal{W}^k \right\}.$$

Then the k -sparse vector $Z_k^\#(u) := u \circ w^*(u)$ is called the optimal k -thresholding of u , and $Z_k^\#(\cdot)$ is called the optimal k -thresholding operator.

The two lemmas below will be used for the analysis in Sections 3 and 4.

Lemma 1 [27] *Let $u \in \mathbb{R}^n$, $v \in \mathbb{R}^m$, $W \subseteq N$ and $t \in N$.*

(i) *If $|W \cup \text{supp}(u)| \leq t$, then*

$$\left\| \left[(I - A^T A)u \right]_W \right\|_2 \leq \delta_t \|u\|_2.$$

(ii) *If $|W| \leq t$, then*

$$\left\| (A^T v)_W \right\|_2 \leq \sqrt{1 + \delta_t} \|v\|_2.$$

Lemma 2 [46] *Let $\{a^p\} \subseteq \mathbb{R}$ ($p = 0, 1, \dots$) be a nonnegative sequence satisfying*

$$a^{p+1} \leq b_1 a^p + b_2 a^{p-1} + b_3$$

for $p \geq 1$, where b_1, b_2 and $b_3 \geq 0$ are constants and $b_1 + b_2 < 1$. Then

$$a^p \leq \theta^{p-1} \left(a^1 + (\theta - b_1) a^0 \right) + \frac{b_3}{1 - \theta}$$

for $p \geq 2$, where $0 \leq \theta < 1$ is a constant given by $\theta = (b_1 + \sqrt{b_1^2 + 4b_2})/2 < 1$.

2.3 Algorithms

Given iterates x^{p-1} and x^p , the heavy-ball search direction is defined as

$$d^p = \alpha A^T (y - Ax^p) + \beta (x^p - x^{p-1}),$$

where $\alpha > 0$ and $\beta \geq 0$ are two parameters. We use the optimal k -thresholding operator $Z_k^\#(\cdot)$ to generate the new iterate x^{p+1} , i.e.,

$$x^{p+1} = Z_k^\#(x^p + d^p),$$

which is called the heavy-ball-based optimal k -thresholding (HBOT) algorithm. Combining HBOT and orthogonal projection (i.e., the least squares problem (2.4) below) leads to the heavy-ball-based optimal k -thresholding pursuit (HBOTP) algorithm. HBOT and HBOTP can be seen as the multi-step extensions of the OT and OTP algorithms in [56, 58]. The two algorithms are formally described as follows.

HBOT and HBOTP algorithms. Input the data (A, y, k) and two initial points x^0 and x^1 . Choose the parameters $\alpha > 0$ and $\beta \geq 0$.

S1 At x^p , set

$$u^p = x^p - \alpha A^T (Ax^p - y) + \beta (x^p - x^{p-1}). \quad (2.2)$$

S2 Solve the optimization problem

$$w^* = \arg \min_w \{ \|y - A(u^p \circ w)\|_2^2 : \mathbf{e}^T w = k, w \in \{0, 1\}^n \}. \quad (2.3)$$

S3 Generate the next iterate x^{p+1} as follows:

For HBOT, let $x^{p+1} = u^p \circ w^*$.

For HBOTP, let $S^{p+1} = \text{supp}(u^p \circ w^*)$ and x^{p+1} be the solution to the least squares problem

$$x^{p+1} = \arg \min_{x \in \mathbb{R}^n} \{\|y - Ax\|_2^2 : \text{supp}(x) \subseteq S^{p+1}\}. \quad (2.4)$$

Repeat S1-S3 above until a certain stopping criterion is met.

In general, the computational cost for solving the binary optimization problem (2.3) is usually high [12, 16]. Replacing (2.3) by its convex relaxation

$$\arg \min_w \left\{ \|y - A(u \circ w)\|_2^2 : w \in \mathcal{P}^k \right\}$$

yields the next heavy-ball-based relaxed optimal k -thresholding (HBROT ω) and the heavy-ball-based relaxed optimal k -thresholding pursuit (HBROTP ω) algorithms, where ω represents the times of solving such a convex relaxation problem at each iteration (which, as pointed out in [56], can be interpreted as the times of data compression within each iteration). As $\omega = 1$, we simply use HBROT and HBROTP to denote the algorithms HBROT1 and HBROTP1, respectively. Clearly, when $\alpha = 1$ and $\beta = 0$, HBROT ω and HBROTP ω reduce, respectively, to ROT ω and ROTP ω in [58].

HBROT ω and HBROTP ω algorithms. Input the data (A, y, k) , two initial points x^0, x^1 and ω . Choose the parameters $\alpha > 0$ and $\beta \geq 0$.

S1 At x^p , calculate u^p by (2.2).

S2 Set $v \leftarrow u^p$. Perform the following loops to produce the vectors $w^{(j)}$ ($j = 1, \dots, \omega$):

for $j = 1 : \omega$ **do**

$$w^{(j)} = \arg \min_w \{\|y - A(v \circ w)\|_2^2 : \mathbf{e}^T w = k, \quad 0 \leq w \leq \mathbf{e}\}, \quad (2.5)$$

and set $v \leftarrow v \circ w^{(j)}$.

end

S3 Let $x^\sharp = \mathcal{H}_k(u^p \circ w^{(1)} \circ \dots \circ w^{(\omega)})$. Generate the next iterate x^{p+1} as follows:

For HBROT ω , let $x^{p+1} = x^\sharp$.

For HBROTP ω , let $S^{p+1} = \text{supp}(x^\sharp)$, and x^{p+1} be the solution to the least squares problem

$$x^{p+1} = \arg \min_{x \in \mathbb{R}^n} \{\|y - Ax\|_2^2 : \text{supp}(x) \subseteq S^{p+1}\}. \quad (2.6)$$

Repeat S1-S3 above until a certain stopping criterion is met.

The choice of stopping criterions depends on the application scenarios. For instance, one can simply prescribe the maximum number of iterations, p_{\max} , which allows the algorithm to perform a total of p_{\max} iterations. One can also terminate the algorithm when $\|y - Ax^p\|_2 \leq \varepsilon$, where $\varepsilon > 0$ is a prescribed tolerance depending on the noise level.

Remark 1 The common feature of the proposed algorithms and existing hard-type thresholding algorithms is that the solutions generated by the algorithms depend on the input value of k , which reflects the user's interest in reconstructing how many significant components of the target signal x^* whose sparsity level is denoted by k^* . In many scenarios, one needs to reconstruct only a few largest components in magnitude of the target signal, instead of the whole signal. In such cases, the user is free to set the desired number k for the proposed algorithms. The quality of reconstruction depends on the input value of k . In fact, the main theorems established in later sections imply that under the RIP of certain order \widehat{k} , the solution generated by the algorithms is the best k -term approximation to the true signal x^* when $k < k^*$, and it coincides with x^* when k satisfies that $k^* \leq k < \widehat{k}$. When $k \geq \widehat{k}$, there would be no guarantee for the proposed algorithms (including existing ones) to recover the signal. If the user expects to reconstruct the whole signal as possible, some information from theory and numerical experiments might be useful for the choice of k . For instance, we may choose k as follows.

- 1) The prior information on the sparsity level k^* of the signal might be available in some situations. In this case, just set $k = k^*$.
- 2) It is well known that the signal can be very likely to be recovered by a certain algorithm if its sparsity level k^* is lower than the half of the spark of the measurement matrix in $\mathbb{R}^{m \times n}$ [25]. So it makes sense to choose $k < (m + 1)/2$ since the spark is bounded above by $m + 1$.
- 3) A large body of simulations and applications indicate that many algorithms work well when the sparsity level of signal is lower than $m/3$, and many such signals can be generally reconstructed by some existing algorithms. Thus it is also reasonable to set $k \leq m/3$ in the proposed algorithms in order to achieve a better chance for the signal to be recovered.
- 4) The number k can be also suggested by experiments including the phase transition of algorithms which sheds light on certain relation between the factors (k, m, n) and the recovery success of signals by given algorithms.

Remark 2 Since x^{p-1}, x^p are two k -sparse vectors in \mathbb{R}^n and $A \in \mathbb{R}^{m \times n}$, the computations of Ax^p and $\beta(x^p - x^{p-1})$ in (2.2) need at most mk and $2k$ multiplication operations, respectively. Thus S1 in HBROTP ω requires at most $mn + m + mk + 2k$ multiplication operations. As pointed out in [58, Section 5.1], S2 and S3 in HBROTP ω requires $O(n^{3.5}L + n \log k) + (mk^2 + k^3/3)$ flops, in which L is the length of the problem data encoding in binary. Since $k \ll m$, the computational complexity of HBROTP ω at each iteration is about $O(n^{3.5}L + mn + n \log k + mk^2)$.

3 Analysis of HBOT and HBOTP

In this section, we establish the error bounds for HBOT and HBOTP under the RIP of order k or $k + 1$. Taking into account the noise influence, the error bound provides the estimation of the distance between the problem solution and the iterates generated by the algorithms. Thus the error bound is an important measurement of the quality of iterates as the approximation to the true solution of the linear inverse problem. In noiseless situations, the error bound implies the global convergence of the algorithms under the RIP assumption. Let us first introduce the following property, which is a combination of Lemmas 3.3 and 3.6 in [58].

Lemma 3 [58] *Let z be a $(2k)$ -sparse vector. Then $\|Az\|_2^2 \geq (1 - 2\delta_k - \delta_{k+s(k)})\|z\|_2^2$ where*

$$s(k) = \begin{cases} 1, & \text{if } k \text{ is an odd number,} \\ 0, & \text{if } k \text{ is an even number.} \end{cases} \quad (3.1)$$

Note that Lemma 3.4 in [58] was established for the sparsity level k being an even number. We now establish the similar result even when k is odd.

Lemma 4 *Let $h, z \in \mathbb{R}^n$ be two k -sparse vectors, and let $\hat{w} \in \mathcal{W}^k$ be any k -sparse binary vector satisfied $\text{supp}(h) \subseteq \text{supp}(\hat{w})$, then*

$$\|[(I - A^T A)(h - z)] \circ \hat{w}\|_2 \leq \sqrt{5}\delta_{k+s(k)}\|h - z\|_2, \quad (3.2)$$

where $s(k)$ is given by (3.1).

Proof For given vectors h, z, \hat{w} satisfying the conditions of the lemma, from [58, Lemma 3.4], we get

$$\|[(I - A^T A)(h - z)] \circ \hat{w}\|_2 \leq \sqrt{5}\delta_k\|h - z\|_2 \quad (3.3)$$

for even number k . Therefore, we just need to show that (3.2) also holds when k is an odd number.

Indeed, assume that k is an odd number. Taking a $(k+1)$ -sparse binary vector $\bar{w} \in \mathcal{W}^{k+1}$ such that $\text{supp}(\hat{w}) \subseteq \text{supp}(\bar{w})$, we obtain

$$\begin{aligned} \|[(I - A^T A)(h - z)] \circ \hat{w}\|_2 &= \left\| \left[(I - A^T A)(h - z) \right]_{\text{supp}(\hat{w})} \right\|_2 \\ &\leq \left\| \left[(I - A^T A)(h - z) \right]_{\text{supp}(\bar{w})} \right\|_2 \\ &= \|[(I - A^T A)(h - z)] \circ \bar{w}\|_2. \end{aligned} \quad (3.4)$$

As h and z are two k -sparse vectors, they are also $(k+1)$ -sparse vectors. Since $\text{supp}(h) \subseteq \text{supp}(\hat{w}) \subseteq \text{supp}(\bar{w})$, and since $k+1$ is even (when k is odd), applying (3.3) to this case yields

$$\|[(I - A^T A)(h - z)] \circ \bar{w}\|_2 \leq \sqrt{5}\delta_{k+1}\|h - z\|_2. \quad (3.5)$$

Combining (3.4) and (3.5), we obtain

$$\|[(I - A^T A)(h - z)] \circ \hat{w}\|_2 \leq \sqrt{5}\delta_{k+1}\|h - z\|_2$$

for odd number k . We conclude that (3.2) holds for any positive integer k . \square

The main results for HBOT and HBOTP are summarized as follows.

Theorem 1 *Let $x \in \mathbb{R}^n$ be a solution to the system $y = Ax + \nu$ where ν is a noise vector. Assume that the RIC, $\delta_{k+s(k)}$, of A and the parameters α, β in HBOT and HBOTP satisfy that $\delta_{k+s(k)} < \gamma^*$ and*

$$0 \leq \beta < \frac{1 + 1/\eta}{1 + \sqrt{5}\delta_{k+s(k)}} - 1, \quad \frac{1 + 2\beta - 1/\eta}{1 - \sqrt{5}\delta_{k+s(k)}} < \alpha < \frac{1 + 1/\eta}{1 + \sqrt{5}\delta_{k+s(k)}}, \quad (3.6)$$

where γ^* (≈ 0.2274) is the unique root of the equation $5\gamma^3 + 5\gamma^2 + 3\gamma - 1 = 0$ in the interval $(0, 1)$, $s(k)$ is given by (3.1) and $\eta := \sqrt{\frac{1+\delta_k}{1-2\delta_k-\delta_{k+s(k)}}}$. Then the sequence $\{x^p\}$ generated by HBOT or HBOTP obeys

$$\|x_S - x^p\|_2 \leq C_1\theta^{p-1} + C_2\|\nu'\|_2, \quad (3.7)$$

where $S := \mathcal{L}_k(x)$, $\nu' := \nu + Ax_{\bar{S}}$, and the quantities C_1, C_2 are defined as

$$C_1 = \|x_S - x^1\|_2 + (\theta - b)\|x_S - x^0\|_2, \quad C_2 = \frac{2 + (1 + \delta_k)\alpha}{(1 - \theta)\sqrt{1 - 2\delta_k - \delta_{k+s(k)}}}, \quad (3.8)$$

and $\theta := (b + \sqrt{b^2 + 4\eta\beta})/2 < 1$ is ensured under the conditions (3.6) and the constant b is given by

$$b := \eta \left(|1 + \beta - \alpha| + \sqrt{5}\alpha\delta_{k+s(k)} \right). \quad (3.9)$$

Proof From (2.2), we have

$$u^p - x_S = (1 - \alpha + \beta)(x^p - x_S) + \alpha(I - A^T A)(x^p - x_S) - \beta(x^{p-1} - x_S) + \alpha A^T \nu', \quad (3.10)$$

where $S = \mathcal{L}_k(x)$ and $\nu' = \nu + Ax_{\bar{S}}$. Let $\hat{w} \in \mathcal{W}^k$ be a k -sparse binary vector such that $\text{supp}(x_S) \subseteq \text{supp}(\hat{w})$. Then $x_S = x_S \circ \hat{w}$. Since $(x_S - u^p) \circ \hat{w}$ is a k -sparse vector and $y = Ax_S + \nu'$, we have

$$\begin{aligned} \|y - A(u^p \circ \hat{w})\|_2 &= \|A(x_S - u^p \circ \hat{w}) + \nu'\|_2 \\ &\leq \|A[(x_S - u^p) \circ \hat{w}]\|_2 + \|\nu'\|_2 \\ &\leq \sqrt{1 + \delta_k} \|(x_S - u^p) \circ \hat{w}\|_2 + \|\nu'\|_2, \end{aligned} \quad (3.11)$$

where the last inequality is obtained by using (2.1). From (3.10), one has

$$\begin{aligned} &\|(x_S - u^p) \circ \hat{w}\|_2 \\ &\leq |1 - \alpha + \beta| \cdot \|(x^p - x_S) \circ \hat{w}\|_2 + \alpha \|(I - A^T A)(x^p - x_S) \circ \hat{w}\|_2 \\ &\quad + \beta \|(x^{p-1} - x_S) \circ \hat{w}\|_2 + \alpha \|(A^T \nu') \circ \hat{w}\|_2. \end{aligned} \quad (3.12)$$

Since x_S, x^p, \hat{w} are k -sparse vectors and $\text{supp}(x_S) \subseteq \text{supp}(\hat{w})$, by using Lemmas 4 and 1 (ii), we obtain

$$\|(I - A^T A)(x^p - x_S) \circ \hat{w}\|_2 \leq \sqrt{5}\delta_{k+s(k)} \|x^p - x_S\|_2 \quad (3.13)$$

and

$$\|(A^T \nu') \circ \hat{w}\|_2 = \left\| (A^T \nu')_{\text{supp}(\hat{w})} \right\|_2 \leq \sqrt{1 + \delta_k} \|\nu'\|_2. \quad (3.14)$$

Substituting (3.13) and (3.14) into (3.12) yields

$$\begin{aligned} \|(x_S - u^p) \circ \hat{w}\|_2 &\leq |1 - \alpha + \beta| \cdot \|x^p - x_S\|_2 + \alpha\sqrt{5}\delta_{k+s(k)} \|x^p - x_S\|_2 \\ &\quad + \beta \|x^{p-1} - x_S\|_2 + \alpha\sqrt{1 + \delta_k} \|\nu'\|_2 \\ &= (|1 + \beta - \alpha| + \sqrt{5}\alpha\delta_{k+s(k)}) \|x^p - x_S\|_2 + \beta \|x^{p-1} - x_S\|_2 \\ &\quad + \alpha\sqrt{1 + \delta_k} \|\nu'\|_2. \end{aligned}$$

It follows from (3.11) that

$$\begin{aligned} \|y - A(u^p \circ \hat{w})\|_2 &\leq \sqrt{1 + \delta_k} \left(|1 + \beta - \alpha| + \sqrt{5}\alpha\delta_{k+s(k)} \right) \|x^p - x_S\|_2 \\ &\quad + \beta\sqrt{1 + \delta_k} \|x^{p-1} - x_S\|_2 + [1 + (1 + \delta_k)\alpha] \|\nu'\|_2. \end{aligned} \quad (3.15)$$

Since $x^{p+1} = u^p \circ w^*$ in HBOT or x^{p+1} is the optimal solution of (2.4) in HBOTP, the sequence $\{x^p\}$ generated by HBOT or HBOTP satisfies

$$\|y - Ax^{p+1}\|_2 \leq \|y - A(u^p \circ w^*)\|_2 \leq \|y - A(u^p \circ w)\|_2 \quad (3.16)$$

for all $w \in \mathcal{W}^k$, where the second inequality follows from (2.3). For $\hat{w} \in \mathcal{W}^k$, it follows from (3.16) that

$$\|y - Ax^{p+1}\|_2 \leq \|y - A(u^p \circ \hat{w})\|_2. \quad (3.17)$$

As $x_S - x^{p+1}$ is a $(2k)$ -sparse vector, by using Lemma 3, one has

$$\begin{aligned} \|y - Ax^{p+1}\|_2 &= \|A(x_S - x^{p+1}) + \nu'\|_2 \\ &\geq \|A(x_S - x^{p+1})\|_2 - \|\nu'\|_2 \\ &\geq \sqrt{1 - 2\delta_k - \delta_{k+s(k)}} \|x_S - x^{p+1}\|_2 - \|\nu'\|_2. \end{aligned} \quad (3.18)$$

Combining (3.15), (3.17) and (3.18) yields

$$\begin{aligned} \|x^{p+1} - x_S\|_2 &\leq \eta(|1 + \beta - \alpha| + \sqrt{5}\alpha\delta_{k+s(k)}) \|x^p - x_S\|_2 + \eta\beta \|x^{p-1} - x_S\|_2 \\ &\quad + \frac{2 + (1 + \delta_k)\alpha}{\sqrt{1 - 2\delta_k - \delta_{k+s(k)}}} \|\nu'\|_2 \\ &= b \|x^p - x_S\|_2 + \eta\beta \|x^{p-1} - x_S\|_2 + (1 - \theta)C_2 \|\nu'\|_2, \end{aligned} \quad (3.19)$$

where η, b, θ, C_2 are given exactly as in Theorem 1. Since $\delta_k \leq \delta_{k+s(k)} < \gamma^*$, we have

$$\eta\sqrt{5}\delta_{k+s(k)} = \sqrt{5}\delta_{k+s(k)} \sqrt{\frac{1 + \delta_k}{1 - 2\delta_k - \delta_{k+s(k)}}} < \sqrt{5}\gamma^* \sqrt{\frac{1 + \gamma^*}{1 - 3\gamma^*}} = 1,$$

where the last equality follows from the fact that γ^* is the root of $5\gamma^3 + 5\gamma^2 + 3\gamma = 1$ in $(0, 1)$. It implies that $0 < \frac{1+1/\eta}{1+\sqrt{5}\delta_{k+s(k)}} - 1$, which shows that the range of β in (3.6) is well defined. Furthermore, the first inequality in (3.6) implies that

$$\frac{1 + 2\beta - 1/\eta}{1 - \sqrt{5}\delta_{k+s(k)}} < 1 + \beta < \frac{1 + 1/\eta}{1 + \sqrt{5}\delta_{k+s(k)}},$$

which indicates that the range for α in (3.6) is also well defined. Combining (3.9) with (3.6), we deduce that

$$\begin{aligned} b &= \eta \left(|1 + \beta - \alpha| + \sqrt{5}\alpha\delta_{k+s(k)} \right) \\ &= \begin{cases} \eta [1 + \beta - \alpha(1 - \sqrt{5}\delta_{k+s(k)})], & \text{if } \frac{1+2\beta-1/\eta}{1-\sqrt{5}\delta_{k+s(k)}} < \alpha \leq 1 + \beta, \\ \eta [-1 - \beta + \alpha(1 + \sqrt{5}\delta_{k+s(k)})], & \text{if } 1 + \beta < \alpha < \frac{1+1/\eta}{1+\sqrt{5}\delta_{k+s(k)}}, \end{cases} \\ &< 1 - \eta\beta, \end{aligned}$$

which means that the relation (3.19) obeys the conditions of Lemma 2. It follows from Lemma 2 that (3.7) holds with $\theta = \frac{b + \sqrt{b^2 + 4\eta\beta}}{2} < 1$ and C_1, C_2 are given by (3.8). \square

The error bound (3.7) indicates that the iterate x^p generated by the algorithms can approximate x_S , the significant components of the solution to the linear inverse problem. In particular, we immediately obtain the following convergence result for the algorithms.

Corollary 1 *Let $x \in \mathbb{R}^n$ be a k -sparse solution to the system $y = Ax$. Assume that the RIC, $\delta_{k+s(k)}$, of A and the parameters α, β in HBOT and HBOTP satisfy the conditions of Theorem 1. Then the sequence $\{x^p\}$ generated by HBOT or HBOTP obeys that $\|x - x^p\|_2 \leq C_1\theta^{p-1}$, where the constant C_1 is defined in Theorem 1. Thus the sequence $\{x^p\}$ generated by HBOT or HBOTP converges to x .*

4 Analysis of HBROT ω and HBROTP ω

In this section, we establish the error bounds for HBROT ω and HBROTP ω . The analysis is far from being trivial. We need a few useful technical results before we actually establish the error bounds. We first recall a helpful lemma concerning the polytope \mathcal{P}^k , which is the special case of Lemma 4.2 with $\tau = k$ in [58].

Lemma 5 [58] *Given an index set $\Lambda \subseteq N$ and a vector $w \in \mathcal{P}^k$, decompose w_Λ as the sum of k -sparse vectors: $w_\Lambda = \sum_{j=1}^q w_{\Lambda_j}$, where $q := \lceil \frac{|\Lambda|}{k} \rceil$, $\Lambda = \bigcup_{j=1}^q \Lambda_j$ and $\Lambda_1 := \mathcal{L}_k(w_\Lambda)$, $\Lambda_2 := \mathcal{L}_k(w_{\Lambda \setminus \Lambda_1})$ and so on. Then*

$$\sum_{j=1}^q \|w_{\Lambda_j}\|_\infty < 2.$$

We now give an inequality concerning the norms $\|\cdot\|_2$, $\|\cdot\|_1$ and $\|\cdot\|_\infty$. This inequality is a modification of Lemma 6.14 in [28], but tailored to the need of the later analysis in this paper.

Lemma 6 *Let $h \in \mathbb{R}^r \setminus \{0\}$ be a vector with $r \geq 2$, and let $\zeta_1 > \zeta_2$ be two positive numbers such that $\|h\|_1 \leq \zeta_1$ and $\|h\|_\infty \leq \zeta_2$. Then*

$$\|h\|_2 \leq \begin{cases} g(r), & \text{if } r \leq t_0, \\ \min\{g(t_0), g(t_0 + 1)\}, & \text{if } r \geq t_0 + 1, \end{cases} \quad (4.1)$$

where $t_0 := \lfloor \frac{4\zeta_1}{\zeta_2} \rfloor$ and

$$g(j) := \frac{1}{\sqrt{j}}\zeta_1 + \frac{\sqrt{j}}{4}\zeta_2, \quad j \in (0, +\infty), \quad (4.2)$$

is strictly decreasing in the interval $(0, \frac{4\zeta_1}{\zeta_2}]$ and strictly increasing in the interval $[\frac{4\zeta_1}{\zeta_2}, +\infty)$.

Proof Without loss of generality, we assume that h is a nonnegative vector. Sort the components of h into descending order, and denote such ordered components by $z_1 \geq z_2 \geq \dots \geq z_r \geq 0$ and $z = (z_1, \dots, z_r)^T$. Thus, $\|z\|_q = \|h\|_q$ for $q \geq 1$. For a given positive integer s and $a_1 \geq a_2 \geq \dots \geq a_s \geq 0$, from [28, Lemma 6.14], one has

$$\sqrt{a_1^2 + \dots + a_s^2} \leq \frac{a_1 + \dots + a_s}{\sqrt{s}} + \frac{\sqrt{s}}{4}(a_1 - a_s). \quad (4.3)$$

There are only two cases according to the relation between r and t_0 .

Case 1. $r \leq t_0$. By using (4.2) and (4.3), we have

$$\|z\|_2 \leq \frac{\|z\|_1}{\sqrt{r}} + \frac{\sqrt{r}}{4}(z_1 - z_r) \leq \frac{\|z\|_1}{\sqrt{r}} + \frac{\sqrt{r}}{4}\|z\|_\infty \leq \frac{1}{\sqrt{r}}\zeta_1 + \frac{\sqrt{r}}{4}\zeta_2 = g(r). \quad (4.4)$$

Case 2. $r \geq t_0 + 1$. Denote by $t := \arg \min_j \{g(j) : j = t_0, t_0 + 1\}$ and let r_1, r_2 be nonnegative integers such that $r = r_1 t + r_2$ ($0 \leq r_2 < t$). Decompose z as the sum of t -sparse vectors: $z = \sum_{j=1}^{r_1+1} z_{Q_j}$, where $Q_j := \{(j-1)t + 1, \dots, jt\}$ with $j = 1, \dots, r_1$, and $Q_{r_1+1} := \{r_1 t + 1, \dots, r_1 t + r_2\}$.

Firstly, we consider the case $r_2 > 0$. With the aid of (4.3), we see that

$$\|z_{Q_j}\|_2 \leq \frac{\|z_{Q_j}\|_1}{\sqrt{t}} + \frac{\sqrt{t}}{4}(z_{(j-1)t+1} - z_{jt}), \quad j = 1, \dots, r_1, \quad (4.5)$$

and

$$\|z_{Q_{r_1+1}}\|_2 \leq \frac{\|z_{Q_{r_1+1}}\|_1}{\sqrt{t}} + \frac{\sqrt{t}}{4}z_{r_1 t + 1}, \quad (4.6)$$

which is ensured under the conditions $a_1 = z_{r_1 t + 1}, \dots, a_{r_2} = z_{r_1 t + r_2}$ and $a_{r_2+1} = \dots = a_t = 0$. Merging (4.5) with (4.6), one has

$$\|z\|_2 = \left\| \sum_{j=1}^{r_1+1} z_{Q_j} \right\|_2 \leq \sum_{j=1}^{r_1+1} \|z_{Q_j}\|_2 \leq \frac{1}{\sqrt{t}} \sum_{j=1}^{r_1+1} \|z_{Q_j}\|_1 + \frac{\sqrt{t}}{4} \mu$$

with

$$\mu := \sum_{j=1}^{r_1} (z_{(j-1)t+1} - z_{jt}) + z_{r_1 t + 1} = z_1 - \sum_{j=1}^{r_1} (z_{jt} - z_{jt+1}) \leq z_1,$$

where the inequality is resulted from $z_1 \geq z_2 \geq \dots \geq z_r$. It follows that

$$\|z\|_2 \leq \frac{1}{\sqrt{t}}\|z\|_1 + \frac{\sqrt{t}}{4}z_1 \leq \frac{1}{\sqrt{t}}\zeta_1 + \frac{\sqrt{t}}{4}\zeta_2 = g(t), \quad (4.7)$$

where the second inequality is ensured by $\|z\|_1 = \|h\|_1 \leq \zeta_1$ and $z_1 = \|h\|_\infty \leq \zeta_2$.

Secondly, we now consider the case $r_2 = 0$, which means $Q_{r_1+1} = \emptyset$ and $z = \sum_{j=1}^{r_1} z_{Q_j}$. Hence, by using (4.3), we obtain

$$\|z\|_2 \leq \sum_{j=1}^{r_1} \|z_{Q_j}\|_2 \leq \frac{1}{\sqrt{t}} \sum_{j=1}^{r_1} \|z_{Q_j}\|_1 + \frac{\sqrt{t}}{4} \sum_{j=1}^{r_1} (z_{(j-1)t+1} - z_{jt}). \quad (4.8)$$

For $z_1 \geq z_2 \geq \dots \geq z_r \geq 0$, we have

$$\sum_{j=1}^{r_1} (z_{(j-1)t+1} - z_{jt}) = z_1 - \sum_{j=1}^{r_1-1} (z_{jt} - z_{jt+1}) - z_{r_1} \leq z_1 = \|z\|_\infty. \quad (4.9)$$

Merging (4.8) with (4.9) leads to

$$\|z\|_2 \leq \frac{1}{\sqrt{t}}\|z\|_1 + \frac{\sqrt{t}}{4}\|z\|_\infty \leq \frac{1}{\sqrt{t}}\zeta_1 + \frac{\sqrt{t}}{4}\zeta_2 = g(t). \quad (4.10)$$

Combining (4.4), (4.7), (4.10) with $\|z\|_q = \|h\|_q (q \geq 1)$, we obtain the relation (4.1) directly. \square

Now, we use an example to show that the upper bound of $\|h\|_2$ in Lemma 6 is tighter than that of Lemma 6.14 in [28] in some situations.

Example 1 Let $h = (1, \epsilon_1, \dots, \epsilon_{14}, \epsilon_0)^T \in \mathbb{R}^{16}$, where $\epsilon_j \geq \epsilon_0$ ($j = 1, \dots, 14$), $\sum_{j=1}^{14} \epsilon_j = 1 - \epsilon_0$ and $\epsilon_0 \in (0, 1/15]$. Hence, $\|h\|_1 = 2$ and $\|h\|_\infty = 1$. Set $\zeta_1 = 2$ and $\zeta_2 = 1$. Then $t_0 = \frac{4\zeta_1}{\zeta_2} = 8$. The upper bound of $\|h\|_2$ can be given by $\|h\|_2 \leq 1.5 - \epsilon_0$ in (4.3) and $\|h\|_2 \leq g(8) = \sqrt{2}$ in (4.1), respectively. Since $1.5 - \epsilon_0 > \sqrt{2}$ for $\epsilon_0 \in (0, 1/15]$, we see that the upper bound of $\|h\|_2$ given by (4.1) is tighter than that of (4.3) if $r > t_0 + 1$ and $\epsilon_0 = \min_{1 \leq i \leq r} |h_i|$ is small enough.

Taking $h = (\|w_{A_1}\|_\infty, \dots, \|w_{A_q}\|_\infty)^T$ with $q = \lceil \frac{|A|}{k} \rceil$, by using Lemma 5, we have $\|h\|_1 < 2$ and $\|h\|_\infty = \|w_{A_1}\|_\infty \leq 1$. Hence, by setting $\zeta_1 = 2$ and $\zeta_2 = 1$, we get $t_0 = 8$ in Lemma 6. This results in the following corollary.

Corollary 2 Under the conditions of Lemma 5, one has $\left(\sum_{j=1}^q \|w_{A_j}\|_\infty^2\right)^{1/2} \leq \xi_q$, where

$$\xi_q = \begin{cases} 1, & \text{if } q = 1, \\ \frac{2}{\sqrt{q}} + \frac{\sqrt{q}}{4}, & \text{if } 2 \leq q < 8, \\ \sqrt{2}, & \text{if } q \geq 8, \end{cases} \quad (4.11)$$

which is strictly decreasing in the interval $[2, 8]$ and $\max_{q \geq 1} \xi_q = \xi_2 = \frac{5}{4}\sqrt{2}$.

Using Lemmas 5 and 6, we can establish the next lemma.

Lemma 7 Let $x \in \mathbb{R}^n$ be a vector satisfying $y = Ax + \nu$ where ν is a noise vector. Let $S = \mathcal{L}_k(x)$ and let $V \subseteq N$ be any given index set such that $S \subseteq V$. At the iterate x^p , the vectors $w^{(j)}$, $j = 1, \dots, \omega$, are generated by HBROT ω or HBROT $P\omega$. For every $i \in \{1, \dots, \omega\}$, we have

$$\begin{aligned} \Theta^i &:= \left\| A \left[(x^p - x_S) \circ w_H^{(i)} \right]_{\overline{V}} \right\|_2 \\ &\leq \sqrt{1 + \delta_k} \left[(\xi_q |1 - \alpha + \beta| + 2\alpha\delta_{3k}) \|x^p - x_S\|_2 + \beta\xi_q \|x^{p-1} - x_S\|_2 \right. \\ &\quad \left. + 2\alpha\sqrt{1 + \delta_k} \|\nu'\|_2 \right], \end{aligned} \quad (4.12)$$

where $w_H^{(i)}$ is the Hadamard product of vectors $w^{(j)}$ ($j = 1, \dots, i$), i.e.,

$$w_H^{(i)} := w^{(1)} \circ w^{(2)} \circ \dots \circ w^{(i)}, \quad i = 1, \dots, \omega, \quad (4.13)$$

and ξ_q is given by (4.11) with $q = \lceil \frac{n-|V|}{k} \rceil$.

Proof Taking $w = w^{(1)}$ and $\Lambda = \bar{V}$ in Lemma 5 and Corollary 2, one has

$$\sum_{j=1}^q \|(w^{(1)})_{\Lambda_j}\|_{\infty} < 2, \quad \sqrt{\sum_{j=1}^q \|(w^{(1)})_{\Lambda_j}\|_{\infty}^2} \leq \xi_q, \quad (4.14)$$

where $q = \lceil \frac{n-|V|}{k} \rceil$ and the definition of Λ_j , $j = 1, \dots, q$, can be found in Lemma 5. Next, we derive the relation (4.12) for given $i \in \{1, \dots, \omega\}$. Define the k -sparse vectors $z^{(l)} := [(u^p - x_S) \circ w_H^{(i)}]_{\Lambda_l}$, $l = 1, \dots, q$, where u^p and $w_H^{(i)}$ are given by (2.2) and (4.13), respectively. Since $w^{(j)} \in \mathcal{P}^k$ ($j = 1, \dots, \omega$), we have

$$\|z^{(l)}\|_2 \leq \|(w_H^{(i)})_{\Lambda_l}\|_{\infty} \cdot \|(u^p - x_S)_{\Lambda_l}\|_2 \leq \|(w^{(1)})_{\Lambda_l}\|_{\infty} \cdot \|(u^p - x_S)_{\Lambda_l}\|_2, \quad (4.15)$$

where the second inequality follows from (4.13) and $0 \leq w^{(j)} \leq \mathbf{e}$ for $j = 1, \dots, \omega$. Since $z^{(l)}$, $l = 1, \dots, q$, are k -sparse vectors, from the definition of Θ^i in (4.12) and (4.15), we obtain

$$\begin{aligned} \Theta^i &= \left\| A \sum_{l=1}^q z^{(l)} \right\|_2 \leq \sum_{l=1}^q \|A z^{(l)}\|_2 \leq \sqrt{1 + \delta_k} \sum_{l=1}^q \|z^{(l)}\|_2 \\ &\leq \sqrt{1 + \delta_k} \sum_{l=1}^q \|(w^{(1)})_{\Lambda_l}\|_{\infty} \cdot \|(u^p - x_S)_{\Lambda_l}\|_2, \end{aligned} \quad (4.16)$$

where the second inequality is given by (2.1). Since $|\Lambda_l| \leq k$ and $|\text{supp}(x^p - x_S) \cup \Lambda_l| \leq 3k$ for $l = 1, \dots, q$, by using (3.10) and Lemma 1, we have

$$\begin{aligned} \|(u^p - x_S)_{\Lambda_l}\|_2 &\leq |1 - \alpha + \beta| \cdot \|(x^p - x_S)_{\Lambda_l}\|_2 + \alpha \|(I - A^T A)(x^p - x_S)\|_{\Lambda_l} \\ &\quad + \beta \|(x^{p-1} - x_S)_{\Lambda_l}\|_2 + \alpha \|(A^T \nu')_{\Lambda_l}\|_2 \\ &\leq |1 - \alpha + \beta| \cdot \|(x^p - x_S)_{\Lambda_l}\|_2 + \alpha \delta_{3k} \|x^p - x_S\|_2 \\ &\quad + \beta \|(x^{p-1} - x_S)_{\Lambda_l}\|_2 + \alpha \sqrt{1 + \delta_k} \|\nu'\|_2. \end{aligned} \quad (4.17)$$

Substituting (4.17) into (4.16) yields

$$\begin{aligned} \frac{\Theta^i}{\sqrt{1 + \delta_k}} &\leq |1 - \alpha + \beta| \cdot \sum_{l=1}^q \|(w^{(1)})_{\Lambda_l}\|_{\infty} \cdot \|(x^p - x_S)_{\Lambda_l}\|_2 \\ &\quad + \alpha \delta_{3k} \sum_{l=1}^q \|(w^{(1)})_{\Lambda_l}\|_{\infty} \cdot \|x^p - x_S\|_2 \\ &\quad + \beta \sum_{l=1}^q \|(w^{(1)})_{\Lambda_l}\|_{\infty} \cdot \|(x^{p-1} - x_S)_{\Lambda_l}\|_2 \\ &\quad + \alpha \sqrt{1 + \delta_k} \sum_{l=1}^q \|(w^{(1)})_{\Lambda_l}\|_{\infty} \cdot \|\nu'\|_2. \end{aligned}$$

It follows from Cauchy-Schwarz inequality and (4.14) that

$$\begin{aligned}
& \frac{\Theta^i}{\sqrt{1 + \delta_k}} \\
& \leq |1 - \alpha + \beta| \sqrt{\sum_{l=1}^q \|(w^{(1)})_{A_l}\|_\infty^2} \sqrt{\sum_{l=1}^q \|(x^p - x_S)_{A_l}\|_2^2 + 2\alpha\delta_{3k}\|x^p - x_S\|_2} \\
& \quad + \beta \sqrt{\sum_{l=1}^q \|(w^{(1)})_{A_l}\|_\infty^2} \sqrt{\sum_{l=1}^q \|(x^{p-1} - x_S)_{A_l}\|_2^2 + 2\alpha\sqrt{1 + \delta_k}\|\nu'\|_2} \\
& \leq |1 - \alpha + \beta|\xi_q\|x^p - x_S\|_2 + 2\alpha\delta_{3k}\|x^p - x_S\|_2 + \beta\xi_q\|x^{p-1} - x_S\|_2 \\
& \quad + 2\alpha\sqrt{1 + \delta_k}\|\nu'\|_2,
\end{aligned}$$

where the last inequality follows from the relation $\sum_{j=1}^q \|z_{A_j}\|_2^2 = \|z_{\bar{V}}\|_2^2 \leq \|z\|_2^2$ for any $z \in \mathbb{R}^n$ due to $\bar{V} = \bigcup_{j=1}^q A_j$ and $A_j \cap A_l = \emptyset$ for $j \neq l$. Thus (4.12) holds. \square

We now estimate the term $\|y - A(u^p \circ w_H^{(\omega)})\|_2$ by using Lemma 7.

Lemma 8 *Let $x \in \mathbb{R}^n$ be a vector satisfying $y = Ax + \nu$ where ν is a noise vector. At the iterate x^p , the vectors u^p and $w^{(j)}$ ($j = 1, \dots, \omega$) are generated by HBROT ω or HBROT $P\omega$. Then*

$$\begin{aligned}
& \|y - A(u^p \circ w_H^{(\omega)})\|_2 \\
& \leq c_{1,q}\sqrt{1 + \delta_k}\|x^p - x_S\|_2 + \sqrt{1 + \delta_k}\beta[\xi_q(\omega - 1) + 1]\|x^{p-1} - x_S\|_2 \\
& \quad + [\alpha(2\omega - 1)(1 + \delta_k) + 1]\|\nu'\|_2,
\end{aligned} \tag{4.18}$$

where $w_H^{(\omega)}$ is given by (4.13), $S := \mathcal{L}_k(x)$, $q = \lceil \frac{n-k}{k} \rceil$, ξ_q is given by (4.11) and $c_{1,q}$ is given as

$$c_{1,q} := (\xi_q(\omega - 1) + 1)|1 - \alpha + \beta| + \alpha(2(\omega - 1)\delta_{3k} + \delta_{2k}). \tag{4.19}$$

Proof Let $\hat{w} \in \mathcal{W}^k$ be a binary vector satisfying $\text{supp}(x_S) \subseteq \text{supp}(\hat{w})$ and $V = \text{supp}(\hat{w})$. From Lemma 4.3 in [58], we get

$$\|y - A[u^p \circ w_H^{(\omega)}]\|_2 \leq \|y - A(u^p \circ \hat{w})\|_2 + \sum_{i=1}^{\omega-1} \left\| A \left[(u^p - x_S) \circ w_H^{(i)} \circ (\mathbf{e} - \hat{w}) \right] \right\|_2, \tag{4.20}$$

where $w_H^{(i)}$, $i = 1, \dots, \omega$, are given by (4.13). As $V = \text{supp}(\hat{w})$ and $|V| = k$, it follows from (4.12) that

$$\begin{aligned}
& \left\| A \left[(u^p - x_S) \circ w_H^{(i)} \circ (\mathbf{e} - \hat{w}) \right] \right\|_2 = \left\| A \left[(u^p - x_S) \circ w_H^{(i)} \right]_{\text{supp}(\hat{w})} \right\|_2 \\
& \leq \sqrt{1 + \delta_k} \left[(\xi_q|1 - \alpha + \beta| + 2\alpha\delta_{3k})\|x^p - x_S\|_2 + \beta\xi_q\|x^{p-1} - x_S\|_2 \right. \\
& \quad \left. + 2\alpha\sqrt{1 + \delta_k}\|\nu'\|_2 \right],
\end{aligned} \tag{4.21}$$

where $q = \lceil \frac{n-k}{k} \rceil$ and $i = 1, \dots, \omega - 1$. We now estimate the term $\|y - A(u^p \circ \widehat{w})\|_2$ in (4.20). Because $|\text{supp}(x^p - x_S) \cup \text{supp}(\widehat{w})| \leq 2k$, by using (3.12) and Lemma 1, we obtain

$$\begin{aligned} & \|(x_S - u^p) \circ \widehat{w}\|_2 \\ & \leq |1 - \alpha + \beta| \cdot \|x^p - x_S\|_2 + \alpha \left\| \left[(I - A^T A)(x^p - x_S) \right]_{\text{supp}(\widehat{w})} \right\|_2 \\ & \quad + \beta \|x^{p-1} - x_S\|_2 + \alpha \left\| (A^T \nu')_{\text{supp}(\widehat{w})} \right\|_2 \\ & \leq (|1 - \alpha + \beta| + \alpha \delta_{2k}) \|x^p - x_S\|_2 + \beta \|x^{p-1} - x_S\|_2 + \alpha \sqrt{1 + \delta_k} \|\nu'\|_2. \end{aligned}$$

It follows from (3.11) that

$$\begin{aligned} \|y - A(u^p \circ \widehat{w})\|_2 & \leq \sqrt{1 + \delta_k} \left[(|1 - \alpha + \beta| + \alpha \delta_{2k}) \|x^p - x_S\|_2 \right. \\ & \quad \left. + \beta \|x^{p-1} - x_S\|_2 + \alpha \sqrt{1 + \delta_k} \|\nu'\|_2 \right] + \|\nu'\|_2. \end{aligned} \quad (4.22)$$

Combining (4.21), (4.22) with (4.20) yields (4.18). \square

The following property of the hard thresholding operator $\mathcal{H}_k(\cdot)$ is shown in [58, Lemma 4.1].

Lemma 9 [58] *Let $z, h \in \mathbb{R}^n$ be two vectors and $\|h\|_0 \leq k$. Then*

$$\|h - \mathcal{H}_k(z)\|_2 \leq \|(z - h)_{S \cup S^*}\|_2 + \|(z - h)_{S^* \setminus S}\|_2,$$

where $S := \text{supp}(h)$ and $S^* := \text{supp}(\mathcal{H}_k(z))$.

Let us state a fundamental property of the orthogonal projection in the following lemma, which can be found in [27, Eq.(3.21)] and [56, p.49], and was extended to the general case in [60, Lemma 4.2].

Lemma 10 [27, 56, 60] *Let $x \in \mathbb{R}^n$ be a vector satisfying $y = Ax + \nu$ where ν is a noise vector. Let $S^* \subseteq N$ be an index set satisfying $|S^*| \leq k$ and*

$$z^* = \arg \min_{z \in \mathbb{R}^n} \{\|y - Az\|_2^2 : \text{supp}(z) \subseteq S^*\}.$$

Then

$$\|z^* - x_S\|_2 \leq \frac{1}{\sqrt{1 - (\delta_{2k})^2}} \|(z^* - x_S)_{S^*}\|_2 + \frac{\sqrt{1 + \delta_k}}{1 - \delta_{2k}} \|\nu'\|_2,$$

where $S := \mathcal{L}_k(x)$ and $\nu' := \nu + Ax_{\bar{S}}$.

We now establish the error bounds for HBROT $_{\omega}$ and HBROT P_{ω} .

Theorem 2 *Suppose that $n > 3k$ and denote $\sigma := \lceil \frac{n-2k}{k} \rceil$. Let $x \in \mathbb{R}^n$ be a vector satisfying $y = Ax + \nu$ where ν is a noise vector. Denote*

$$t_k := \frac{\sqrt{1 + \delta_k}}{\sqrt{1 - \delta_{2k}}}, \quad z_k := \sqrt{1 - \delta_{2k}^2}. \quad (4.23)$$

- (i) Assume that the $(3k)$ -th order RIC, δ_{3k} , of the matrix A and the nonnegative parameters (α, β) satisfy $\delta_{3k} < \gamma^*(\omega)$ and

$$\beta < \frac{1-d_1}{1+d_1+d_2}, \quad \frac{(d_0+d_2+2)\beta+d_0}{d_0-d_1+1} < \alpha < \frac{d_0+2-(d_2-d_0)\beta}{d_0+d_1+1}, \quad (4.24)$$

where $\gamma^*(\omega)$ is the unique root of the equation $G_\omega(\gamma) = 1$ in the interval $(0, 1)$, where

$$G_\omega(\gamma) := (2\omega+1)\gamma\sqrt{\frac{1+\gamma}{1-\gamma}} + \gamma, \quad (4.25)$$

and the constants d_0, d_1, d_2 are given as

$$\begin{cases} d_0 := t_k(\omega\xi_\sigma + 1), \\ d_1 := t_k(2\omega\delta_{3k} + \delta_{2k}) + \delta_{3k}, \\ d_2 := t_k[\xi_\sigma(\omega-1) + 1] \frac{2\omega\delta_{3k} + \delta_{2k}}{2(\omega-1)\delta_{3k} + \delta_{2k}}. \end{cases} \quad (4.26)$$

Then, the sequence $\{x^p\}$ produced by HBROT ω obeys

$$\|x^p - x_S\|_2 \leq \theta_1^{p-1} \left[\|x^1 - x_S\|_2 + (\theta_1 - b_1)\|x^0 - x_S\|_2 \right] + \frac{b_3}{1-\theta_1} \|\nu'\|_2 \quad (4.27)$$

with $\theta_1 := \frac{b_1 + \sqrt{b_1^2 + 4b_2}}{2}$. The fact $\theta_1 < 1$ is ensured under (4.24) and b_1, b_2, b_3 are given as

$$\begin{aligned} b_1 &:= t_k c_\sigma + (|1 + \beta - \alpha| + \alpha\delta_{3k}), \quad b_2 := \beta t_k [\xi_\sigma(\omega-1) + 1] \frac{c_\sigma}{c_{1,\sigma}} + \beta, \\ b_3 &:= \frac{\alpha(2\omega-1)(1+\delta_k) + 2}{\sqrt{1-\delta_{2k}}} \cdot \frac{2\delta_{3k}}{2(\omega-1)\delta_{3k} + \delta_{2k}} \cdot \frac{c_\sigma}{c_\sigma - c_{1,\sigma}} + \alpha\sqrt{1+\delta_k}, \end{aligned} \quad (4.28)$$

where $c_{1,\sigma}$ and ξ_σ are given by (4.19) and (4.11), respectively, and

$$c_\sigma := (\omega\xi_\sigma + 1)|1 - \alpha + \beta| + \alpha(2\omega\delta_{3k} + \delta_{2k}). \quad (4.29)$$

- (ii) Suppose that the $(3k)$ -th order RIC, δ_{3k} , of the matrix A and the nonnegative parameters (α, β) satisfy $\delta_{3k} < \gamma^\sharp(\omega)$ and

$$\beta < \frac{z_k - d_1}{1 + d_1 + d_2}, \quad \frac{(d_0 + d_2 + 2)\beta + d_0 + 1 - z_k}{d_0 - d_1 + 1} < \alpha < \frac{d_0 + 1 + z_k - (d_2 - d_0)\beta}{d_0 + d_1 + 1}, \quad (4.30)$$

where the constants d_0, d_1, d_2 are given by (4.26) and $\gamma^\sharp(\omega)$ is the unique root of the equation $\frac{1}{\sqrt{1-\gamma^2}}G_\omega(\gamma) = 1$ in the interval $(0, 1)$, where $G_\omega(\gamma)$ is given by (4.25).

Then, the sequence $\{x^p\}$ produced by HBROT $P\omega$ obeys

$$\begin{aligned} \|x^p - x_S\|_2 &\leq \theta_2^{p-1} \left[\|x^1 - x_S\|_2 + \left(\theta_2 - \frac{b_1}{z_k}\right)\|x^0 - x_S\|_2 \right] \\ &\quad + \frac{1}{1-\theta_2} \left(\frac{b_3}{z_k} + \frac{\sqrt{1+\delta_k}}{1-\delta_{2k}} \right) \|\nu'\|_2 \end{aligned} \quad (4.31)$$

with $\theta_2 := \frac{b_1 + \sqrt{b_1^2 + 4b_2 z_k}}{2z_k}$. The fact $\theta_2 < 1$ is ensured under (4.30) and the constants $b_i (i = 1, 2, 3)$ and z_k are given by (4.28) and (4.23), respectively.

Proof Let $x^\sharp = \mathcal{H}_k(u^p \circ w_H^{(\omega)})$ be generated by the Algorithms, where $w_H^{(\omega)}$ is given by (4.13). By using Lemma 9, we have

$$\|x_S - x^\sharp\|_2 \leq \|(u^p \circ w_H^{(\omega)} - x_S)_{X \cup S}\|_2 + \|(u^p \circ w_H^{(\omega)} - x_S)_{X \setminus S}\|_2, \quad (4.32)$$

where $X = \text{supp}(x^\sharp)$. Using (3.10) and the triangle inequality, we have that

$$\begin{aligned} \|(u^p \circ w_H^{(\omega)} - x_S)_{X \setminus S}\|_2 &= \|[(u^p - x_S) \circ w_H^{(\omega)}]_{X \setminus S}\|_2 \leq \|(u^p - x_S)_{X \setminus S}\|_2 \\ &\leq |1 - \alpha + \beta| \cdot \|(x^p - x_S)_{X \setminus S}\|_2 + \alpha \|(I - A^T A)(x^p - x_S)_{X \setminus S}\|_2 \\ &\quad + \beta \|(x^{p-1} - x_S)_{X \setminus S}\|_2 + \alpha \|(A^T \nu')_{X \setminus S}\|_2, \end{aligned}$$

where the first equality is ensured by $(x_S)_{X \setminus S} = 0$ and the first inequality is due to (4.13) and $0 \leq w^{(j)} \leq \mathbf{e}$ for $j = 1, \dots, \omega$. Since $|X \setminus S| \leq k$ and $|\text{supp}(x^p - x_S) \cup (X \setminus S)| \leq 3k$, by using Lemma 1, we see that

$$\begin{aligned} \|(u^p \circ w_H^{(\omega)} - x_S)_{X \setminus S}\|_2 &\leq (|1 + \beta - \alpha| + \alpha \delta_{3k}) \|x^p - x_S\|_2 \\ &\quad + \beta \|x^{p-1} - x_S\|_2 + \alpha \sqrt{1 + \delta_k} \|\nu'\|_2. \end{aligned} \quad (4.33)$$

Denote

$$\Theta_1 := \|A(u^p \circ w_H^{(\omega)} - x_S)_{X \cup S}\|_2, \quad \Theta_2 := \|A(u^p \circ w_H^{(\omega)} - x_S)_{\overline{X \cup S}}\|_2. \quad (4.34)$$

As $|X \cup S| \leq 2k$, by using (2.1), we obtain

$$\Theta_1 \geq \sqrt{1 - \delta_{2k}} \|(u^p \circ w_H^{(\omega)} - x_S)_{X \cup S}\|_2. \quad (4.35)$$

For any given $\zeta \in (0, 1)$, we consider the following two cases associated with Θ_1 and Θ_2 .

Case 1. $\Theta_2 \leq \zeta \Theta_1$. Since $y = Ax_S + \nu'$, by the triangle inequality and (4.34), we have

$$\begin{aligned} \|y - A(u^p \circ w_H^{(\omega)})\|_2 &= \|A(u^p \circ w_H^{(\omega)} - x_S) - \nu'\|_2 \\ &= \|A(u^p \circ w_H^{(\omega)} - x_S)_{X \cup S} + A(u^p \circ w_H^{(\omega)} - x_S)_{\overline{X \cup S}} - \nu'\|_2 \\ &\geq \Theta_1 - \Theta_2 - \|\nu'\|_2 \\ &\geq (1 - \zeta)\Theta_1 - \|\nu'\|_2. \end{aligned} \quad (4.36)$$

Merging (4.35), (4.36) with (4.18) yields

$$\begin{aligned} &\|(u^p \circ w_H^{(\omega)} - x_S)_{X \cup S}\|_2 \\ &\leq \frac{1}{(1 - \zeta)\sqrt{1 - \delta_{2k}}} (\|y - A(u^p \circ w_H^{(\omega)})\|_2 + \|\nu'\|_2) \\ &\leq \frac{t_k c_{1, q_1}}{1 - \zeta} \|x^p - x_S\|_2 + \frac{\beta t_k}{1 - \zeta} [\xi_{q_1} (\omega - 1) + 1] \|x^{p-1} - x_S\|_2 \\ &\quad + \frac{\alpha(2\omega - 1)(1 + \delta_k) + 2}{(1 - \zeta)\sqrt{1 - \delta_{2k}}} \|\nu'\|_2, \end{aligned} \quad (4.37)$$

where $q_1 = \lceil \frac{n-k}{k} \rceil = \sigma + 1$ and t_k, c_{1, q_1} are given in (4.23) and (4.19), respectively.

Case 2. $\theta_2 > \zeta\theta_1$. From (4.34) and (4.35), we obtain

$$\|(u^p \circ w_H^{(\omega)} - x_S)_{X \cup S}\|_2 \leq \frac{1}{\zeta\sqrt{1-\delta_{2k}}} \|A[(u^p - x_S) \circ w_H^{(\omega)}]_{\overline{X \cup S}}\|_2. \quad (4.38)$$

Taking $V = X \cup S$ and $i = \omega$ in (4.12), one has

$$\begin{aligned} & \|A[(u^p - x_S) \circ w_H^{(\omega)}]_{\overline{X \cup S}}\|_2 \\ & \leq \sqrt{1+\delta_k} \left[c_{2,q_2} \|x^p - x_S\|_2 + \beta \xi_{q_2} \|x^{p-1} - x_S\|_2 + 2\alpha\sqrt{1+\delta_k} \|\nu'\|_2 \right] \end{aligned} \quad (4.39)$$

with $q_2 = \lceil \frac{n-|X \cup S|}{k} \rceil \geq \sigma$ which is due to $|X \cup S| \leq 2k$, and c_{2,q_2} is defined as

$$c_{2,q_2} := \xi_{q_2} |1 - \alpha + \beta| + 2\alpha\delta_{3k}. \quad (4.40)$$

Substituting (4.39) into (4.38), we get

$$\begin{aligned} \|(u^p \circ w_H^{(\omega)} - x_S)_{X \cup S}\|_2 & \leq \frac{t_k}{\zeta} [c_{2,q_2} \|x^p - x_S\|_2 + \beta \xi_{q_2} \|x^{p-1} - x_S\|_2 \\ & \quad + 2\alpha\sqrt{1+\delta_k} \|\nu'\|_2]. \end{aligned} \quad (4.41)$$

From (4.11), we see that ξ_q is decreasing in $[2, n]$. For $q_1 = \sigma + 1$ and $q_2 \geq \sigma \geq 2$, we have $\xi_{q_1}, \xi_{q_2} \leq \xi_\sigma$. It follows from (4.19) and (4.40) that $c_{1,q_1} \leq c_{1,\sigma}$ and $c_{2,q_2} \leq c_{2,\sigma}$. Combining (4.37) and (4.41) leads to

$$\begin{aligned} & \|(u^p \circ w_H^{(\omega)} - x_S)_{X \cup S}\|_2 \\ & \leq t_k \max \left\{ \frac{c_{1,\sigma}}{1-\zeta}, \frac{c_{2,\sigma}}{\zeta} \right\} \|x^p - x_S\|_2 \\ & \quad + \beta t_k \max \left\{ \frac{\xi_\sigma(\omega-1)+1}{1-\zeta}, \frac{\xi_\sigma}{\zeta} \right\} \|x^{p-1} - x_S\|_2 \\ & \quad + \frac{1}{\sqrt{1-\delta_{2k}}} \max \left\{ \frac{\alpha(2\omega-1)(1+\delta_k)+2}{1-\zeta}, \frac{2\alpha(1+\delta_k)}{\zeta} \right\} \|\nu'\|_2 \end{aligned} \quad (4.42)$$

for any $\zeta \in (0, 1)$.

Next, we select a suitable parameter $\zeta \in (0, 1)$ such that the right hand of (4.42) is as small as possible. For $\delta_{2k} \leq \delta_{3k}$ and $\xi_\sigma < 2$ in (4.11), we have

$$\frac{c_{2,\sigma}}{c_{1,\sigma}} = \frac{\xi_\sigma |1 - \alpha + \beta| + 2\alpha\delta_{3k}}{[\xi_\sigma(\omega-1)+1]|1 - \alpha + \beta| + \alpha[2(\omega-1)\delta_{3k} + \delta_{2k}]} \leq \frac{2\delta_{3k}}{2(\omega-1)\delta_{3k} + \delta_{2k}}. \quad (4.43)$$

It is easy to check that

$$\min_{\zeta \in (0,1)} \max \left\{ \frac{c_{1,\sigma}}{1-\zeta}, \frac{c_{2,\sigma}}{\zeta} \right\} = c_{1,\sigma} + c_{2,\sigma} = c_\sigma, \quad (4.44)$$

where c_σ is given by (4.29) and its minimum attains at

$$\zeta^* = \frac{c_{2,\sigma}}{c_{1,\sigma} + c_{2,\sigma}} = \frac{\xi_\sigma |1 - \alpha + \beta| + 2\alpha\delta_{3k}}{(\omega\xi_\sigma + 1)|1 - \alpha + \beta| + \alpha(2\omega\delta_{3k} + \delta_{2k})}. \quad (4.45)$$

That is,

$$\max \left\{ \frac{c_{1,\sigma}}{1-\zeta^*}, \frac{c_{2,\sigma}}{\zeta^*} \right\} = c_\sigma. \quad (4.46)$$

Moreover, noting that $\xi_\sigma < 2$ and $\delta_{2k} \leq \delta_{3k}$, we have $\zeta^* \geq \frac{\xi_\sigma}{\omega\xi_\sigma+1}$. In particular, by taking $\zeta = \zeta^*$ in (4.42), we deduce that

$$\max \left\{ \frac{\xi_\sigma(\omega-1)+1}{1-\zeta^*}, \frac{\xi_\sigma}{\zeta^*} \right\} = \frac{\xi_\sigma(\omega-1)+1}{1-\zeta^*} = \frac{\xi_\sigma(\omega-1)+1}{c_{1,\sigma}} c_\sigma,$$

and

$$\begin{aligned} & \max \left\{ \frac{\alpha(2\omega-1)(1+\delta_k)+2}{1-\zeta^*}, \frac{2\alpha(1+\delta_k)}{\zeta^*} \right\} \\ &= \frac{1}{\zeta^*} \max \left\{ [\alpha(2\omega-1)(1+\delta_k)+2] \frac{\zeta^*}{1-\zeta^*}, 2\alpha(1+\delta_k) \right\} \\ &= \frac{c_\sigma}{c_{2,\sigma}} \max \left\{ [\alpha(2\omega-1)(1+\delta_k)+2] \frac{c_{2,\sigma}}{c_{1,\sigma}}, 2\alpha(1+\delta_k) \right\} \\ &\leq \frac{c_\sigma}{c_{2,\sigma}} \max \left\{ [\alpha(2\omega-1)(1+\delta_k)+2] \frac{2\delta_{3k}}{2(\omega-1)\delta_{3k}+\delta_{2k}}, 2\alpha(1+\delta_k) \right\} \\ &= \left[\alpha(2\omega-1)(1+\delta_k)+2 \right] \frac{2\delta_{3k}}{2(\omega-1)\delta_{3k}+\delta_{2k}} \cdot \frac{c_\sigma}{c_{2,\sigma}}, \end{aligned} \quad (4.47)$$

where the second equality is given by (4.45), the inequality above follows from (4.43), and the last equality holds owing to $\delta_{2k} \leq \delta_{3k}$. Merging (4.42) with (4.46)-(4.47), we obtain

$$\begin{aligned} & \|(u^p \circ w_H^{(\omega)} - x_S)_{X \cup S}\|_2 \\ &\leq t_k c_\sigma \|x^p - x_S\|_2 + \beta t_k \frac{\xi_\sigma(\omega-1)+1}{c_{1,\sigma}} c_\sigma \|x^{p-1} - x_S\|_2 \\ &\quad + \frac{\alpha(2\omega-1)(1+\delta_k)+2}{\sqrt{1-\delta_{2k}}} \cdot \frac{2\delta_{3k}}{2(\omega-1)\delta_{3k}+\delta_{2k}} \cdot \frac{c_\sigma}{c_{2,\sigma}} \|\nu'\|_2. \end{aligned} \quad (4.48)$$

Combining (4.33), (4.48) with (4.32), we have

$$\|x_S - x^\sharp\|_2 \leq b_1 \|x^p - x_S\|_2 + b_2 \|x^{p-1} - x_S\|_2 + b_3 \|\nu'\|_2, \quad (4.49)$$

where the constants b_1, b_2, b_3 are given by (4.28).

Next, we estimate $\|x^{p+1} - x_S\|_2$ for HBROT ω and HBROTP ω based on the relation (4.49).

(i) Since $x^{p+1} = x^\sharp$ in HBROT ω , (4.49) becomes

$$\|x^{p+1} - x_S\|_2 \leq b_1 \|x^p - x_S\|_2 + b_2 \|x^{p-1} - x_S\|_2 + b_3 \|\nu'\|_2. \quad (4.50)$$

Now, we consider the conditions of Lemma 2. Merging (4.43) with (4.44) produces

$$\frac{c_\sigma}{c_{1,\sigma}} \leq \frac{2\omega\delta_{3k} + \delta_{2k}}{2(\omega-1)\delta_{3k} + \delta_{2k}}.$$

It follows from (4.28) and (4.29) that

$$\begin{aligned} b_1 + b_2 &\leq t_k c_\sigma + (|1 + \beta - \alpha| + \alpha\delta_{3k}) \\ &\quad + \left\{ t_k \frac{2\omega\delta_{3k} + \delta_{2k}}{2(\omega-1)\delta_{3k} + \delta_{2k}} [\xi_\sigma(\omega-1) + 1] + 1 \right\} \beta = F(\alpha, \beta), \end{aligned} \quad (4.51)$$

where

$$\begin{aligned} F(\alpha, \beta) &:= (d_0 + 1)|1 - \alpha + \beta| + d_1\alpha + (d_2 + 1)\beta, \\ &= \begin{cases} -(d_0 - d_1 + 1)\alpha + (d_0 + d_2 + 2)\beta + d_0 + 1, & \text{if } \alpha \leq 1 + \beta, \\ (d_0 + d_1 + 1)\alpha + (d_2 - d_0)\beta - (d_0 + 1), & \text{if } \alpha > 1 + \beta, \end{cases} \end{aligned} \quad (4.52)$$

with the constants d_0, d_1, d_2 are given by (4.26).

Based on the fact $\delta_k \leq \delta_{2k} \leq \delta_{3k} < \gamma^*(\omega)$ and the function $G_\omega(\gamma)$ in (4.25) is strictly increasing in the interval $(0, 1)$, by using (4.26), we have

$$d_1 \leq [(2\omega + 1)t_k + 1]\delta_{3k} \leq G_\omega(\delta_{3k}) < G_\omega(\gamma^*(\omega)) = 1, \quad (4.53)$$

which shows that the range of β in (4.24) is well defined. From the first inequality in (4.24), we see that

$$\frac{(d_0 + d_2 + 2)\beta + d_0}{d_0 - d_1 + 1} < 1 + \beta < \frac{d_0 + 2 - (d_2 - d_0)\beta}{d_0 + d_1 + 1}, \quad (4.54)$$

which implies that the range of α in (4.24) is also well defined. Merging (4.52)-(4.54) with the second inequality in (4.24), we see that if $\frac{(d_0 + d_2 + 2)\beta + d_0}{d_0 - d_1 + 1} < \alpha \leq 1 + \beta$, then

$$F(\alpha, \beta) < -(d_0 - d_1 + 1)\frac{(d_0 + d_2 + 2)\beta + d_0}{d_0 - d_1 + 1} + (d_0 + d_2 + 2)\beta + d_0 + 1 = 1,$$

and if $1 + \beta < \alpha < \frac{d_0 + 2 - (d_2 - d_0)\beta}{d_0 + d_1 + 1}$, then

$$F(\alpha, \beta) < (d_0 + d_1 + 1)\frac{d_0 + 2 - (d_2 - d_0)\beta}{d_0 + d_1 + 1} + (d_2 - d_0)\beta - (d_0 + 1) = 1.$$

It follows from (4.51) that $b_1 + b_2 < 1$. Hence, applying Lemma 2 to the relation (4.50), we conclude that (4.27) holds with $\theta_1 = \frac{b_1 + \sqrt{b_1^2 + 4b_2}}{2} < 1$.

(ii) Since x^{p+1} is given by (2.6) and $S^{p+1} = \text{supp}(x^\sharp)$ in HBROTP ω , by setting $S^* = S^{p+1}$ and $z^* = x^{p+1}$ in Lemma 10, we have

$$\begin{aligned} \|x^{p+1} - x_S\|_2 &\leq \frac{1}{z_k} \left\| (x^\sharp - x_S)_{S^{p+1}} \right\|_2 + \frac{\sqrt{1 + \delta_k}}{1 - \delta_{2k}} \|\nu'\|_2 \\ &\leq \frac{1}{z_k} \|x^\sharp - x_S\|_2 + \frac{\sqrt{1 + \delta_k}}{1 - \delta_{2k}} \|\nu'\|_2, \end{aligned} \quad (4.55)$$

where z_k is given in (4.23) and the first inequality follows from the fact $(x^{p+1})_{S^{p+1}} = (x^\sharp)_{S^{p+1}} = 0$. Combining (4.55) with (4.49), we have

$$\|x^{p+1} - x_S\|_2 \leq \frac{b_1}{z_k} \|x^p - x_S\|_2 + \frac{b_2}{z_k} \|x^{p-1} - x_S\|_2 + \left(\frac{b_3}{z_k} + \frac{\sqrt{1 + \delta_k}}{1 - \delta_{2k}} \right) \|\nu'\|_2. \quad (4.56)$$

Similar to the analysis in Part (i), we need to show that $\frac{b_1}{z_k} + \frac{b_2}{z_k} < 1$.

From the conditions of Theorem 2(ii), we have $\delta_{2k} \leq \delta_{3k} < \gamma^\sharp(\omega)$. Since the function $G_\omega(\gamma)$ in (4.25) is strictly increasing in $(0, 1)$, one has

$$d_1 \leq G_\omega(\delta_{3k}) < G_\omega(\gamma^\sharp(\omega)) = \sqrt{1 - (\gamma^\sharp(\omega))^2} < \sqrt{1 - (\delta_{2k})^2} = z_k,$$

where the first inequality is given by (4.53), the first equality follows from the fact that $\gamma^\sharp(\omega)$ is the root of $\frac{1}{\sqrt{1-\gamma^2}}G_\omega(\gamma) = 1$ in $(0, 1)$ and the last equality is given by (4.23). It follows that the range of β in (4.30) is well defined. From the first inequality in (4.30), we derive

$$\frac{(d_0 + d_2 + 2)\beta + d_0 + 1 - z_k}{d_0 - d_1 + 1} < 1 + \beta < \frac{d_0 + 1 + z_k - (d_2 - d_0)\beta}{d_0 + d_1 + 1}, \quad (4.57)$$

which means that the range of α in (4.30) is well defined. Combining (4.52), (4.57) with the second inequality in (4.30) leads to

$$F(\alpha, \beta) < \begin{cases} -(d_0 - d_1 + 1) \frac{(d_0 + d_2 + 2)\beta + d_0 + 1 - z_k}{d_0 - d_1 + 1} + (d_0 + d_2 + 2)\beta + d_0 + 1, \\ \quad \text{if } \frac{(d_0 + d_2 + 2)\beta + d_0 + 1 - z_k}{d_0 - d_1 + 1} < \alpha \leq 1 + \beta, \\ (d_0 + d_1 + 1) \frac{d_0 + 1 + z_k - (d_2 - d_0)\beta}{d_0 + d_1 + 1} + (d_2 - d_0)\beta - (d_0 + 1), \\ \quad \text{if } 1 + \beta < \alpha < \frac{d_0 + 1 + z_k - (d_2 - d_0)\beta}{d_0 + d_1 + 1}, \end{cases}$$

$= z_k.$

It follows from (4.51) that $\frac{b_1}{z_k} + \frac{b_2}{z_k} < 1$. Therefore, by Lemma 2, it follows from (4.56) that (4.31) holds with $\theta_2 = \frac{b_1 + \sqrt{b_1^2 + 4b_2z_k}}{2z_k} < 1$. \square

Remark 3(i) When $\nu = 0$ and x is a k -sparse vector, from (4.27) and (4.31), we observe that the sequence $\{x^p\}$ generated by HBROT ω or HBROTP ω converges to x .

- (ii) The condition $n > 3k$ in Theorem 2 can be removed. If so, the constant ξ_σ will be replaced by $\max_{q \geq 1} \xi_q = \frac{5}{4}\sqrt{2}$ (see Corollary 2). In addition, if $n > 9k$, then $\sigma = \lceil \frac{n-2k}{k} \rceil \geq 8$. In this case, we see from (4.11) that ξ_σ in Theorem 2 can be replaced by $\min_{q \geq 2} \xi_q = \sqrt{2}$.
- (iii) When $\omega = 1$, HBROT ω and HBROTP ω reduce to HBROT and HBROTP, respectively. In this case, the RIP bounds in Theorem 2 are reduced to $\delta_{3k} < \gamma^*(1) \approx 0.2118$ for HBROT and $\delta_{3k} < \gamma^\sharp(1) \approx 0.2079$ for HBROTP.
- (iv) It is not convenient to calculate the RIC of the matrix A and (4.30) is just a sufficient condition for the theoretical performance of HBROTP ω . In practical implementation, the parameters (α, β) in HBROTP may be set as $0 \leq \beta < 1/4$ and $\alpha \geq 1 + \beta$ for simplicity to roughly meet the conditions (4.30).

5 Numerical experiments

Sparse signal and image recovery through measurements $y = Ax + \nu$, where x denotes the signal/image to recover, is a typical linear inverse problem. In this section, we provide some experiment results for the proposed HBROTP algorithm and compare its performance with several existing methods. The experiments in Sections 5.1 and 5.2 are performed on a server with the processor Intel(R) Xeon(R) CPU E5-2680 v3 @ 2.50GHz and 256GB memory, while others are performed on a PC with the processor Intel(R) Core(TM) i7-10700 CPU @ 2.90 GHz and 16 GB memory. All involved convex optimization problems are solved by CVX [30] with

solver ‘*Mosek*’ [2]. The comparison of six algorithms including HBROTP, ROTP2, PGROTP, ℓ_1 -min, OMP and PLB is mainly made via the phase transitions based on synthetic data together with the reconstruction, deblurring and denoising of a few real images.

5.1 Phase transition

The first experiment is carried out to compare the performances of the algorithms except PLB through the phase transition curve (PTC) [5, 6] and average recovery time. All sparse vectors $x^* \in \mathbb{R}^n$ and matrices $A \in \mathbb{R}^{m \times n}$ are randomly generated, and the position of nonzero elements of x^* follows the uniform distribution. In addition, all columns of A are normalized and the entries of A and the nonzeros of x^* are independent and identically distributed random variables following $\mathcal{N}(0, 1)$. In this experiment, we consider both accurate measurements $y = Ax^*$ and inaccurate measurements $y = Ax^* + \epsilon h$ with fixed $n = 1000$, where $\epsilon = 5 \times 10^{-3}$ is the noise level and $h \in \mathbb{R}^m$ is a normalized standard Gaussian noise. We let HBROTP start from $x^1 = x^0 = 0$ with fixed parameters $\alpha = 5$ and $\beta = 0.2$, while other algorithms start from $x^0 = 0$. The maximum number of iterations of HBROTP, ROTP2 and PGROTP is set as 50, while OMP is performed exactly k iterations and ℓ_1 -min is performed by the solver ‘*Mosek*’ directly. Given the random data (A, x^*) or (A, x^*, h) , the recovery is counted as ‘*success*’ when the criterion

$$\|x^p - x^*\|_2 / \|x^*\|_2 \leq 10^{-3}$$

is satisfied, in which x^p is the solution generated by algorithms.

Denote by $\kappa = m/n$ and $\rho = k/m$, where κ is often called the sampling rate or the compression ratio. In the (κ, ρ) -space, the region below the PTC is called the ‘*success*’ recovery region, where the solution of the SLI problem can be exactly or approximately recovered, while the region above the PTC corresponds to the ‘*failure*’ region. Thus if the region below the PTC is wider, the performance of an algorithm would be better. We now briefly describe the mechanism for plotting the PTC which is taken as the classical 50% logistic regression curve, and more detailed information can be found in [5, 6]. To generate the PTCs, 13 groups of $m = \lceil \kappa \cdot n \rceil$ are considered, where the sampling rate κ is ranged from 0.1 to 0.7 with stepsize 0.05. For any given m , by using the bisection method, the approximated recovery phase transition region $[k_{\min}, k_{\max}]$ is produced for each algorithm, in which the success rate of recovery is at least 90% as $k < k_{\min}$ and at most 10% as $k > k_{\max}$. The interval $[k_{\min}, k_{\max}]$ will be equally divided into $\min\{k_{\max} - k_{\min}, 50\}$ parts, and 10 problem instances are tested for each k to produce the recovery success rate for given algorithm. Thus the PTCs can be obtained from the logistic regression model in [5, 6] directly.

The PTCs for the experimented algorithms are shown in Fig. 1(a) and (b), which correspond to the accurate measurements and inaccurate measurements with the noise level $\epsilon = 5 \times 10^{-3}$, respectively. The results indicate that HBROTP has the highest PTC as $\kappa \leq 0.5$, in which case the recovery capability of HBROTP is superior to other algorithms in this experiment. However, the PTCs indicate that ROTP2, PGROTP and OMP may perform relatively better than HBROTP with a larger κ . The comparison in Fig. 1(a) and (b) demonstrates that all algorithms are robust for signal recovery when the measurements are slightly inaccurate except

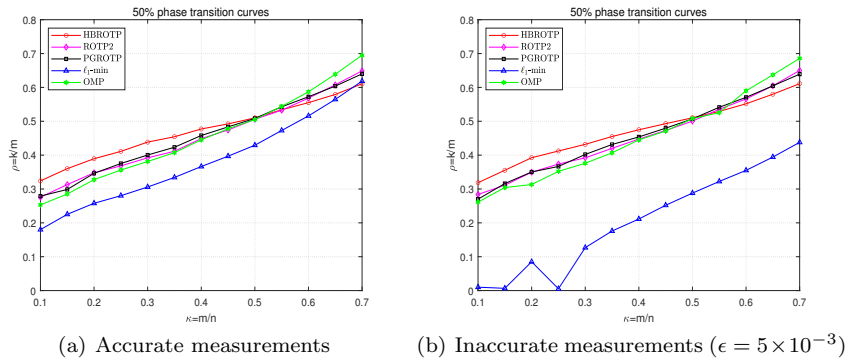


Fig. 1 The 50% success rate phase transition curves for algorithms.

ℓ_1 -min. The comparison indicates that the overall performance of HBROTP is very comparable to those existing methods in this experiment.

In the intersection of the recovery regions of multiple algorithms, we compare the average CPU time for signal recovery via these algorithms. Specifically, for each given κ , we test 10 problem instances for each algorithm with the mesh (κ, ρ) , wherein ρ is ranged from 0.02 to 1 with stepsize 0.02 until the success rate of recovery is less than 90%. The ratios of the average computational time of ROTP2, PGROTP, ℓ_1 -min and OMP against that of HBROTP are displayed in Fig. 2 (a)-(d), respectively. Fig. 2 (a) and (b) show that HBROTP is at least 1.6 times faster than ROTP2 in most areas and slower than PGROTP except in the region $[0.1, 0.2] \times [0.02, 0.1]$. On the other hand, from Fig. 2 (a)-(d), we observe that the ROT-type algorithms including HBROTP, ROTP2 and PGROTP take relatively more time to solve the problems than ℓ_1 -min and OMP, due to solving quadratic convex optimization problems.

5.2 Image reconstruction

In this section, we compare the performances of several algorithms on the reconstruction of several images (*Lena*, *Peppers* and *Baboon*) of size 512×512 . Only accurate measurements are used in the experiment, and the measurement matrices are $m \times n$ normalized standard Gaussian matrices with $n = 512$ and $m = \lceil \kappa \cdot n \rceil$, where κ is the sampling rate. The discrete wavelet transform with the ‘*sym8*’ wavelet is used to establish the sparse representation of the images. The input sparsity level is set as $k = \lceil n/10 \rceil$ for HBROTP, ROTP2 and PGROTP, and the parameters of HBROTP are set as $\alpha = 5$ and $\beta = 0.2$. The peak signal-to-noise ratio (PSNR) is used to compare the reconstruction quality of images, which is defined by

$$PSNR := 10 \cdot \log_{10}(V^2/MSE),$$

where MSE denotes the mean-squared error between the reconstructed and original image, and V represents the maximum fluctuation in the original image data type ($V = 255$ is used in our experiments). Clearly, the larger the value of PSNR, the higher the reconstruction quality.

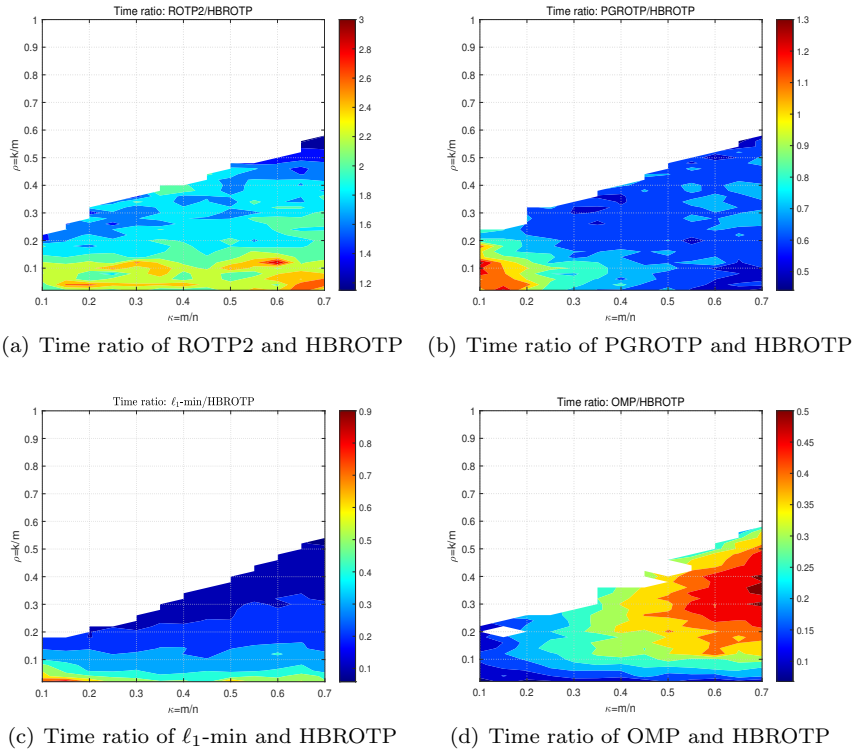


Fig. 2 The ratios of average CPU time of the algorithms.

Table 1 Comparison of PSNR (dB) for algorithms with different sampling rates.

	κ	HBROTP	ROTP2	PGROTP	ℓ_1 -min	OMP
Lena	0.3	32.60	32.34	33.12	33.63	31.37
	0.4	34.37	32.49	31.75	35.10	32.95
	0.5	35.63	33.11	31.93	37.04	34.34
Peppers	0.3	31.31	32.33	33.27	33.03	30.17
	0.4	33.10	31.78	31.60	34.08	31.66
	0.5	34.23	32.04	31.10	35.90	33.38
Baboon	0.3	28.70	31.35	32.33	29.90	28.35
	0.4	29.12	30.06	30.00	30.05	28.53
	0.5	29.37	30.06	30.07	30.20	28.78

The results in terms of PSNR with sampling rates $\kappa = 0.3, 0.4, 0.5$ are summarized in Tab. 1, from which we see that HBROTP is always superior to OMP and inferior to ℓ_1 -min in reconstruction quality. For ROTP-type algorithms with $\kappa = 0.4, 0.5$, the PSNR values of HBROTP exceed that of ROTP2, PGROTP at least 1.88 dB for *Lena* and 1.32 dB for *Peppers*, respectively. In other cases, ROTP2 and PGROTP obtained better results than HBROTP in reconstruction quality. In particular, the performances of ROTP2 and PGROTP are always equivalent or superior to ℓ_1 -min for *Baboon*. In the meantime, the comparison of visual quality for the constructed images by HBROTP with $\kappa = 0.3, 0.4, 0.5$ is displayed in Fig.

3. It can be seen that the reconstruction quality has been significantly improved for three images as the sampling rate κ is ranged from 0.3 to 0.5, and the best visual results have been achieved around $\kappa = 0.5$.

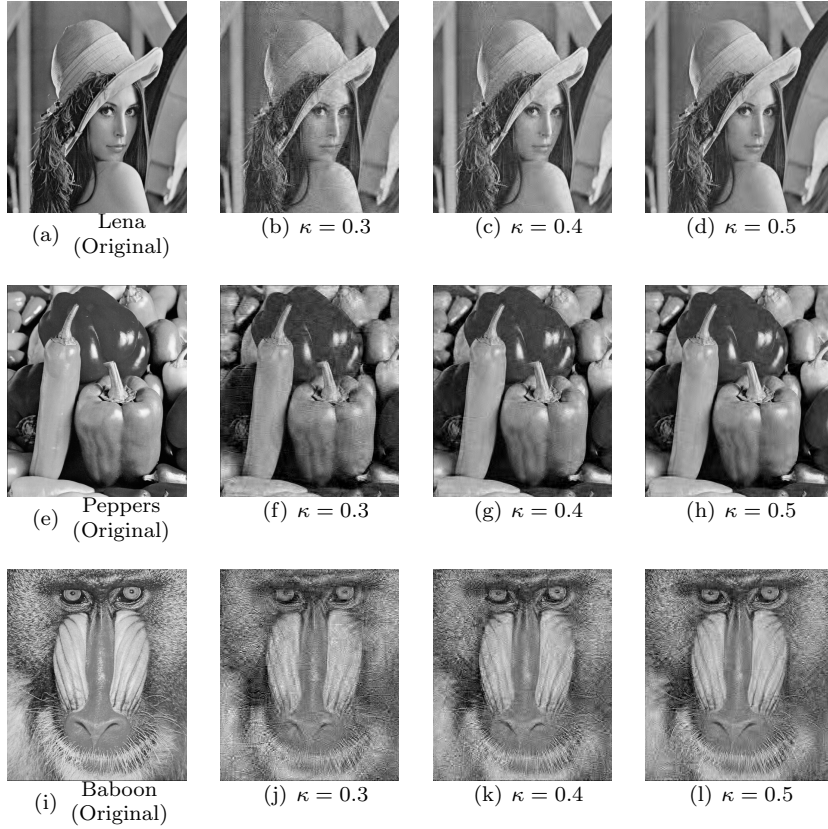


Fig. 3 Performance of HBROTP for three images with different sampling rates.

5.3 Image deblurring and denoising

In this section, we compare the performances of HBROTP and PLB on image deblurring and denoising. In our experiments, several images including *Boats*, *Cam-eraman*, *Clock*, *Goldhill* and *Shepp-Logan* of size 128×128 are expressed as vectors in \mathbb{R}^n with $n = 16384$ through concatenating their columns. For a given image z , the corresponding blurred noisy image $y \in \mathbb{R}^n$ is obtained by (1.1), in which $\Phi \in \mathbb{R}^{n \times n}$ is the blurring matrix generated by a Gaussian kernel `fspecial('Gaussian',11,0.6)` in Matlab with periodic boundary condition (see Chapter 4 in [29]), and ν is a Gaussian white noise vector with mean 0 and standard deviation $\hat{\sigma}$. The sparse representation of z is expressed as $z = \Psi x$, where Ψ is taken as the synthesis operator generated by the linear B-splines [1, 11], denoted Ψ_1 , or the discrete wavelet

matrix generated by the ‘*sym8*’ wavelet, denoted Ψ_2 . Thus the image deblurring and denoising can be achieved by solving the corresponding SLI problem (1.2).

For HBROTP, the discrete wavelet transform, i.e., $\Psi = \Psi_2$ is used to achieve the sparse representation of the image, and the parameters in this algorithm are set as $k = \lceil 0.4n \rceil$, $\alpha = 1$ and $\beta = 0.8$. For PLB, we use PLB_i to represent PLB with $\Psi = \Psi_i$ for $i = 1, 2$, and the parameters (μ, d, δ) are given as follows: $\mu = 0.05$ is determined experimentally in terms of PSNR; the dimension of Krylov subspace is set as $d = 11$ according to the suggestion in [1]; δ is the same as that of [11]. The stopping criterion of the algorithm is given by

$$\|x^{p+1} - x^p\|_2 / \|x^{p+1}\|_2 \leq 10^{-4}.$$

Table 2 Comparison of PSNR (dB) and CPU time (in seconds) of HBROTP and PLB on image deblurring and denoising with different standard deviation $\hat{\sigma}$.

Standard deviation	Images	PSNR(dB)			CPU time(seconds)		
		PLB ₁	PLB ₂	HBROTP	PLB ₁	PLB ₂	HBROTP
$\hat{\sigma} = 2$	Barbara	35.34	35.34	37.75	0.80	4.31	2291
	Boats	35.53	35.52	35.34	0.83	3.30	2049
	Cameraman	35.58	35.57	37.26	0.83	2.80	1383
	Clock	35.66	35.65	38.12	0.59	2.13	1305
	Goldhill	35.34	35.33	35.05	0.70	2.81	2319
	Shepp-Logan	35.54	35.51	38.72	0.86	3.28	1764
$\hat{\sigma} = 4$	Barbara	30.74	30.74	33.86	0.94	4.03	2071
	Boats	30.80	30.80	33.06	0.38	3.11	2411
	Cameraman	30.79	30.79	33.53	0.78	4.14	1370
	Clock	30.90	30.90	33.44	0.53	3.28	1737
	Goldhill	30.76	30.75	33.02	0.80	3.95	2444
	Shepp-Logan	30.93	30.92	33.70	0.61	4.66	1381

The results in terms of CPU time and PSNR for HBROTP and PLB on image deblurring and denoising with two different standard deviations $\hat{\sigma} = 2, 4$ are given in Tab. 2. In the case $\hat{\sigma} = 2$, the PSNR values of HBROTP exceed that of PLB₁ and PLB₂ at least 1.6 dB for all images except *Boats* and *Goldhill*. As the noise intensity increases, the differences of PSNR values between HBROTP and PLB_{*i*} ($i = 1, 2$) are enlarged to 2.2 dB for all images as $\hat{\sigma} = 4$. This experiment shows that HBROTP can be stronger than PLB on image deblurring and denoising, and HBROTP is more stable than PLB in noisy situations. However, solving quadratic subproblem (2.5) causes the HBROTP method to consume more time than PLB₁ and PLB₂. Moreover, PLB₁ is faster than PLB₂ since the synthesis operator Ψ_1 is more sparser than the discrete wavelet matrix Ψ_2 . Finally, the deblurring/denoising effects of HBROTP and PLB₁ on *Cameraman* and *Shepp-Logan* with $\hat{\sigma} = 2$ are shown in Fig. 4, from which it can be observed that both HBROTP and PLB₁ can successfully recover the two images in high quality.

6 Conclusions

The new algorithms that combine the optimal k -thresholding and heavy-ball technique are proposed in this paper. Such algorithms can be seen as the acceleration

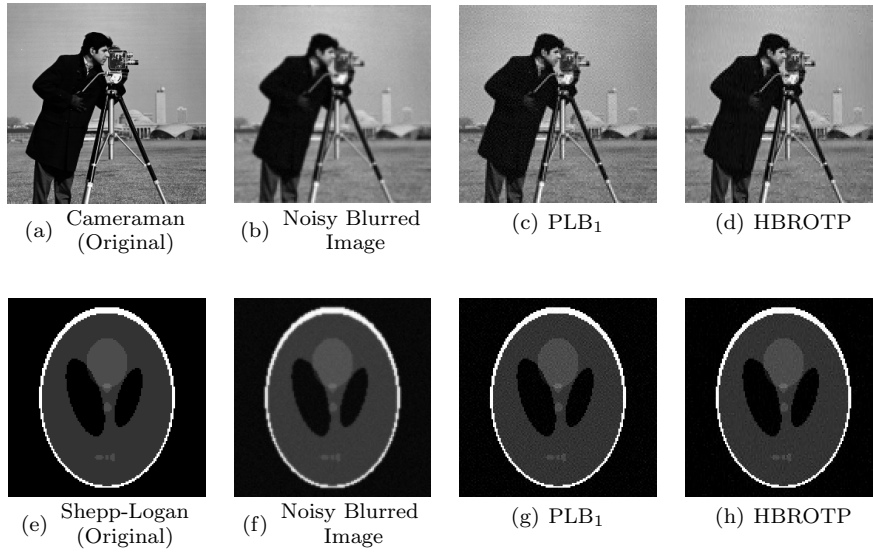


Fig. 4 Performance of PLB_1 and HBROTP on image deblurring and denoising with $\hat{\sigma} = 2$.

versions of the optimal k -thresholding methods. The solution error bounds and convergence of the proposed algorithms have been shown mainly under the RIP of the matrices. The numerical performance of the proposed HBROTP algorithm has been evaluated through phase transition, average runtime and image processing. The experiment results indicate that HBROTP is a robust signal recovery method, especially when the sampling rate is relatively low (e.g., $\kappa \leq 0.5$), and it is generally faster than the standard ROTP method thank to the heavy-ball acceleration technique.

References

1. Alotaibi M., Buccini A., Reichel L.: Krylov subspace split Bregman methods. *Appl. Numer. Math.* 184, 371–390 (2023)
2. Andersen E.D., Andersen K.D.: The MOSEK interior point optimizer for linear programming: an implementation of the homogeneous algorithm. *High performance optimization*. Springer, Boston, MA 33, 197–232 (2000)
3. Aujol J.F., Dossal C., Rondepierre A.: Convergence rates of the heavy-ball method under the Lojasiewicz property. *Math. Program.* 198, 195–254 (2023)
4. Beck A., Teboulle M.: A fast iterative shrinkage-thresholding algorithm for linear inverse problems. *SIAM J. Imaging Sci.* 2(1), 183–202 (2009)
5. Blanchard J.D., Tanner J.: Performance comparisons of greedy algorithms in compressed sensing. *Numer. Linear Algebra Appl.* 22(2), 254–282 (2015)
6. Blanchard J.D., Tanner J., Wei K.: CGIHT: conjugate gradient iterative hard thresholding for compressed sensing and matrix completion. *IMA J. Inf. Inference* 4(4), 289–327 (2015)
7. Blumensath T.: Accelerated iterative hard thresholding. *Signal Process.* 92(3), 752–756 (2012)
8. Blumensath T., Davies M.E.: Iterative thresholding for sparse approximations. *J. Fourier Anal. Appl.* 14, 629–654 (2008)

9. Blumensath T., Davies M.E.: Normalized iterative hard thresholding: Guaranteed stability and performance. *IEEE J. Sel. Top. Signal Process.* 4(2), 298–309 (2010)
10. Borgerding M., Schniter P., Rangan S.: AMP-Inspired deep networks for sparse linear inverse problems. *IEEE Trans. Signal Process.* 65(16), 4293–4308 (2017)
11. Buccini A., Pasha M., Reichel L.: Linearized Krylov subspace Bregman iteration with nonnegativity constraint. *Numer. Algorithms* 87, 1177–1200 (2021)
12. Buchheim C., Traversi E.: Quadratic combinatorial optimization using separable underestimators. *INFORMS J. Comput.* 30(3), 424–437 (2018)
13. Cai Y., Donatelli M., Bianchi D., Huang T.Z.: Regularization preconditioners for frame-based image deblurring with reduced boundary artifacts. *SIAM J. Sci. Comput.* 38(1), B164–B189 (2016)
14. Candès E.J., Tao T.: Decoding by linear programming. *IEEE Trans. Inform. Theory* 51(12), 4203–4215 (2005)
15. Candès E.J., Wakin M.B., Boyd S.P.: Enhancing sparsity by reweighted ℓ_1 -minimization. *J. Fourier Anal. Appl.* 14, 877–905 (2008)
16. Chaovalitwongse W.A., Androulakis I.P., Pardalos P.M.: Quadratic integer programming: Complexity and equivalent forms. In: Floudas C.A., Pardalos P.M.: (eds) *Encyclopedia of Optimization*. Springer, Boston, MA (2008)
17. Chartrand R.: Exact reconstruction of sparse signals via nonconvex minimization. *IEEE Signal Process. Lett.* 14(10), 707–710 (2007)
18. Chen S.S., Donoho D.L., Saunders M.A.: Atomic decomposition by basis pursuit. *SIAM J. Sci. Comput.* 20(1), 33–61 (1998)
19. Chen W., Zhang B., Jin S., Ai B., Zhong Z.: Solving sparse linear inverse problems in communication systems: A deep learning approach with adaptive depth. *IEEE J. Sel. Areas Commun.* 39(1), 4–17 (2021)
20. Dai W., Milenkovic O.: Subspace pursuit for compressive sensing signal reconstruction. *IEEE Trans. Inform. Theory* 55(5), 2230–2249 (2009)
21. Daubechies I., Defrise M., Mol C.De: An iterative thresholding algorithm for linear inverse problems with a sparsity constraint. *Comm. Pure Appl. Math.* 57(11), 1413–1457 (2004)
22. Donoho D.L.: De-noising by soft-thresholding. *IEEE Trans. Inform. Theory* 41(3), 613–627 (1995)
23. Donoho D.L., Johnstone I.M.: Ideal spatial adaptation by wavelet shrinkage. *Biometrika* 81(3), 425–455 (1994)
24. Elad M.: Why simple shrinkage is still relevant for redundant representations? *IEEE Trans. Inform. Theory* 52(12), 5559–5569 (2006)
25. Elad M.: *Sparse and Redundant Representations: From Theory to Applications in Signal and Image Processing*. Springer, New York (2010)
26. Eldar Y.C., Kutyniok G.: *Compressed Sensing: Theory and Applications*. Cambridge University Press, Cambridge (2012)
27. Foucart S.: Hard thresholding pursuit: An algorithm for compressive sensing. *SIAM J. Numer. Anal.* 49(6), 2543–2563 (2011)
28. Foucart S., Rauhut H.: *A Mathematical Introduction to Compressive Sensing*. Springer, New York (2013)
29. Golub G.H., Van Loan C.F.: *Matrix Computations*, 4th ed.. Johns Hopkins University Press, Baltimore (2013)
30. Grant M., Boyd S.: CVX: matlab software for disciplined convex programming. Version 1.21 (2017)
31. Gürbüzbalaban M., Ozdaglar A., Parrilo P.A.: On the convergence rate of incremental aggregated gradient algorithms. *SIAM J. Optim.* 27(2), 1035–1048 (2017)
32. Kuru N., Birbil Ş.İ., Gürbüzbalaban M., Yildirim S.: Differentially private accelerated optimization algorithms. *SIAM J. Optim.* 32(2), 795–821 (2022)
33. Kyrillidis A., Cevher V.: Matrix recipes for hard thresholding methods. *J. Math. Imaging Vision* 48, 235–265 (2014)
34. Lessard L., Recht B., Packard A.: Analysis and design of optimization algorithms via integral quadratic constraints. *SIAM J. Optim.* 26(1), 57–95 (2016)
35. Li S., Amin M., Zhao G., Sun H.: Radar imaging by sparse optimization incorporating MRF clustering prior. *IEEE Geosci. Remote Sens. Lett.* 17(7), 1139–1143 (2020)
36. Li H., Cheng H., Wang Z., Wu G.C.: Distributed Nesterov gradient and heavy-ball double accelerated asynchronous optimization. *IEEE Trans. Neural Netw. Learn. Syst.* 32(12), 5723–5737 (2021)

37. Liu Y., Zhan Z., Cai J.F., Guo D., Chen Z., Qu X.: Projected iterative soft-thresholding algorithm for tight frames in compressed sensing magnetic resonance imaging. *IEEE Trans. Med. Imaging* 35(9), 2130–2140 (2016)
38. Meng N., Zhao Y.B.: Newton-step-based hard thresholding algorithms for sparse signal recovery. *IEEE Trans. Signal Process.* 68, 6594–6606 (2020)
39. Meng N., Zhao Y.B.: Newton-type optimal thresholding algorithms for sparse optimization problems. *J. Oper. Res. Soc. China* 10, 447–469 (2022)
40. Meng N., Zhao Y.B., Kočvara M., Sun Z.F.: Partial gradient optimal thresholding algorithms for a class of sparse optimization problems. *J. Global Optim.* 84, 393–413 (2022)
41. Mohammadi H., Razaviyayn M., Jovanović M.R.: Robustness of accelerated first-order algorithms for strongly convex optimization problems. *IEEE Trans. Automat. Control* 66(6), 2480–2495 (2021)
42. Needell D., Tropp J.A.: CoSaMP: Iterative signal recovery from incomplete and inaccurate samples. *Appl. Comput. Harmon. Anal.* 26(3), 301–321 (2009)
43. Oymak S., Recht B., Soltanolkotabi M.: Sharp time-data tradeoffs for linear inverse problems. *IEEE Trans. Inform. Theory* 64(6), 4129–4158 (2018)
44. Polyak B.T.: Some methods of speeding up the convergence of iteration methods. *USSR Comput. Math. Math. Phys.* 4(5), 1–17 (1964)
45. Schniter P., Potter L.C., Ziniel J.: Fast Bayesian matching pursuit. In: *Proc. Inform. Theory Appl. Workshop* 326–333 (2008)
46. Sun Z.F., Zhou J.C., Zhao Y.B., Meng N.: Heavy-ball-based hard thresholding algorithms for sparse signal recovery. *J. Comput. Appl. Math.* 430, 115264 (2023)
47. Tirer T., Giryes R.: Back-projection based fidelity term for ill-posed linear inverse problems. *IEEE Trans. Image Process.* 29, 6164–6179 (2020)
48. Tropp J.A., Gilbert A.C.: Signal recovery from random measurements via orthogonal matching pursuit. *IEEE Trans. Inform. Theory* 53(12), 4655–4666 (2007)
49. Tropp J.A., Wright S.J.: Computational methods for sparse solution of linear inverse problems. In: *Proc. IEEE* 98(6), 948–958 (2010)
50. Ugrinovskii V., Petersen I.R., Shames I.: Global convergence and asymptotic optimality of the heavy ball method for a class of nonconvex optimization problems. *IEEE Control Syst. Lett.* 6, 2449–2454 (2022)
51. Wipf D.P., Rao B.D.: Sparse Bayesian learning for basis selection. *IEEE Trans. Signal Process.* 52(8), 2153–2164 (2004)
52. Xiang J., Dong Y., Yang Y.: FISTA-net: Learning a fast iterative shrinkage thresholding network for inverse problems in imaging. *IEEE Trans. Med. Imaging* 40(5), 1329–1339 (2021)
53. Xin R., Khan U.A.: Distributed heavy-ball: A generalization and acceleration of first-order methods with gradient tracking. *IEEE Trans. Automat. Control* 65(6), 2627–2633 (2020)
54. Yin W., Osher S., Goldfarb D., Darbon J.: Bregman iterative algorithms for ℓ_1 -minimization with applications to compressed sensing. *SIAM J. Imaging Sci.* 1(1), 143–168 (2008)
55. Yin W.: Analysis and generalizations of the linearized Bregman method. *SIAM J. Imaging Sci.* 3(4), 856–877 (2010)
56. Zhao Y.B.: Optimal k -thresholding algorithms for sparse optimization problems. *SIAM J. Optim.* 30(1), 31–55 (2020)
57. Zhao Y.B., Luo Z.Q.: Constructing new reweighted ℓ_1 -algorithms for the sparsest points of polyhedral sets. *Math. Oper. Res.* 42(1), 57–76 (2017)
58. Zhao Y.B., Luo Z.Q.: Analysis of optimal thresholding algorithms for compressed sensing. *Signal Process.* 187, 108148 (2021)
59. Zhao Y.B., Luo Z.Q.: Natural thresholding algorithms for signal recovery with sparsity. *IEEE Open J. Signal Process.* 3, 417–431 (2022)
60. Zhao Y.B., Luo Z.Q.: Improved RIP-based bounds for guaranteed performance of two compressed sensing algorithms. *Sci. China Math.* 66(5), 1123–1140 (2023)